



23 **Abstract**

24 Precipitation and air temperature are key drivers of watershed models. Currently there are many  
25 open-access gridded precipitation and air temperature datasets at different spatial and temporal  
26 resolutions over global or quasi-global scale. Motivated by the scarcity and substantial temporal  
27 and spatial gaps in ground measurements in Africa, this study evaluated the performance of three  
28 open-access precipitation datasets (i.e. CHIRPS (Climate Hazards Group InfraRed Precipitation  
29 with Station data), TRMM (Tropical Rainfall Measuring Mission) and CFSR (Climate Forecast  
30 System Reanalysis)) and one air temperature dataset (CFSR) in driving Soil and Water  
31 Assessment Tool (SWAT) model in simulation of daily and monthly streamflow in the upper  
32 Gilgel Abay Basin, Ethiopia. The “best” available measurements of precipitation and air  
33 temperature from sparse gauge stations were also used to drive SWAT model and the results  
34 were compared with those using open-access datasets. After a comprehensive comparison of a  
35 total of eight model scenarios with different combinations of precipitation and air temperature  
36 inputs, we draw the following conclusions: (1) using measured precipitation from even sparse  
37 available stations consistently yielded better performance in streamflow simulation than using all  
38 three open-access precipitation datasets; (2) using CFSR air temperature yielded almost identical  
39 performance in streamflow simulation to using measured air temperature from gauge stations; (3)  
40 among the three open-access precipitation, overall CHIRPS yielded best performance. These  
41 results suggested that the CHIRPS precipitation available at high spatial resolution (0.05°)  
42 together with CFSR air temperature can be a promising alternative open-access data source for  
43 streamflow simulation in this data-scarce area in the case of limited access to desirable gauge  
44 data.

45

46 **Keywords:** Blue Nile; Climate Hazards Group InfraRed Precipitation with Station data; Tropical  
47 Rainfall Measuring Mission; Climate Forecast System Reanalysis; SWAT; satellite precipitation

## 48 **1 Introduction**

49 Hydrological models or rainfall-runoff models are essential for understanding the hydrological  
50 processes of river basins and supporting operational management of water resources  
51 characterized with large spatial and temporal variability (Uhlenbrook et al., 2010; Tuo et al.,  
52 2016). Precipitation and air temperature are two necessary weather variables required as inputs to  
53 hydrological models. An accurate representation of the temporal and spatial variability of  
54 precipitation and air temperature is essential for achieving good simulation and prediction of  
55 hydrological processes from models (Wagner et al., 2012; Tuo et al., 2016; Laiti et al., 2018).

56 Ideally a reasonably dense network of gauge stations are needed to obtain the reliable measured  
57 precipitation and air temperature data that are adequate to effectively represent the weather at the  
58 basin scale. In reality, the network of gauge stations is often sparse and the point-based  
59 measurements with limited coverage are insufficient to capture the spatial and temporal  
60 variability of weather variables. Unfortunately, at global scale the number of gauge stations has  
61 been significantly declined. This data availability situation is even worse in developing countries  
62 and remote areas where measurements are not available or even not existent. Sometimes even  
63 data are available, strict data sharing policy could constraint the free access to the public, or the  
64 data quality is very poor. For example, despite the importance of Nile River as vital water  
65 resource for local population, the understanding of hydrology is still quite limited which is  
66 mainly due to the data scarcity and unfavorable data quality (Uhlenbrook et al., 2010; Dile &  
67 Srinivasan, 2014; Roth & Lemann, 2016). Very often we are facing limited availability of in-situ  
68 measurement, which hinders us to do hydrological Prediction in Ungauged Basins (PUB)  
69 (Hrachowitz et al., 2013). Therefore, there is a clear need for improving data collection (if

70 human and financial resources allow) and/or exploring alternative data sources which are more  
71 feasible.

72 Many studies have been conducted to explore the accuracy of using open-access weather data  
73 (most focused on only precipitation data) in driving hydrological models in streamflow  
74 simulation by using available gauge precipitation data as reference. Our current study focuses on  
75 the widely-used Soil and Water Assessment Tool (SWAT) model (Arnold et al., 1998; Arnold &  
76 Fohrer, 2005; Gassman et al., 2007; Song et al., 2011, and more in the SWAT Literature  
77 Database at [https://www.card.iastate.edu/swat\\_articles/](https://www.card.iastate.edu/swat_articles/)). SWAT is also a popular model for  
78 many studies of Nile basin where is overall poorly gauged (see a review by Griensven et al.,  
79 2012). For SWAT community, a common source of weather data (precipitation, air temperature  
80 and other variables) is the Climate Forecast System Reanalysis (CFSR) data. The CFSR data are  
81 promoted and popularized by the SWAT official website through providing ready-to-use weather  
82 data in desired format with the data portal at <http://globalweather.tamu.edu/>. The CFSR is an  
83 interpolated dataset on a 38-km grid using climate forecast system with most available in-situ  
84 data and satellite data (Radcliffe Z & Mukundan, 2017). The readily availability of weather data  
85 in the required format attracted many studies to use CFSR data to drive hydrological models.

86 Several studies evaluated the performance of using CFSR precipitation to drive SWAT in  
87 streamflow simulation. However, contrasting findings were reported from different studies. For  
88 example, using CFSR precipitation was found to yield satisfactory streamflow simulation in  
89 Lake Tana Basin, Ethiopia (Dile & Srinivasan, 2014), in four small watersheds in USA and the  
90 Gumera watershed in Ethiopia (Fuka et al., 2014). But CFSR was found to generate  
91 unsatisfactory streamflow simulation in two upstream watersheds of the Three Gorges Reservoir

92 in China (Yang et al., 2014) and in two watersheds in USA (Radcliffe & Mukundan, 2017). The  
93 latter found that using the PRISM (Parameter-elevation Relationships on Independent Slopes  
94 Model) precipitation data as input yielded satisfactory to even very good streamflow simulation  
95 in the same watersheds. All aforementioned studies only explicitly evaluated the performance of  
96 CFSR precipitation data but did not comprehensively evaluate the other weather variables (e.g.  
97 air temperature) from CFSR. It should be noted that the minimum requirements in weather data  
98 input for SWAT model include daily precipitation and daily air temperature (maximum and  
99 minimum temperature). Then one research question arises: what is the performance of using  
100 CFSR air temperature data together with other better precipitation data to drive SWAT in  
101 streamflow simulation? This is particularly relevant for data-scarce or ungauged basins where  
102 reliable air temperature data from gauge stations are not available or even nonexistent, thereby  
103 hindering the application of SWAT model and other models in such regions. Therefore, this  
104 study aims to answer this research question.

105 Besides the CFSR precipitation data, currently there are many open-access gridded precipitation  
106 datasets at different spatial and temporal resolutions over the global or quasi-global scale (Duan  
107 et al., 2016). A detailed summary of available precipitation datasets can be found in Tapiador et  
108 al., (2012). Overall, the accuracy of different open-access gridded precipitation datasets vary  
109 from region to region and thus evaluation of certain precipitation products in a range of regions  
110 with different characteristics is important for both product developers and users. Such  
111 importance attracted a vast amount of studies that have been carried out to evaluate a single or  
112 multiple precipitation products at scales varying from the quasi-global to basin scales (Awange  
113 et al., 2016; Bitew & Gebremichael, 2011; Duan & Bastiaanssen, 2013a; Duan et al., 2012; Jiang  
114 et al., 2017; Liu et al., 2015; Tan & Duan, 2017; Tang et al., 2016; Yong et al., 2010).

115 Most gridded precipitation datasets are at the spatial resolution of  $0.25^\circ$  with one grid  
116 representing mean precipitation over an area of about  $625 \text{ km}^2$ , thus such datasets cannot  
117 sufficiently reflect the spatial variability of precipitation for relatively small areas. Among them,  
118 the TRMM (Tropical Rainfall Measuring Mission) multi-satellite precipitation analysis (TMPA)  
119 product (Huffman et al., 2007) is one of the most widely used products at  $0.25^\circ$  and has been  
120 used in many applications. It is worth noting that the recently (in 2015) released CHIRPS  
121 (Climate Hazards Group InfraRed Precipitation with Station data) precipitation dataset (Funk et  
122 al., 2015) stands out by providing daily precipitation at the finest spatial resolution of  $0.05^\circ$  (one  
123 grid representing around  $25 \text{ km}^2$ ) from 1981 to present. This high spatial resolution enables it to  
124 better describe the spatial variability of precipitation and favors its application in hydrological  
125 studies at wider scales including the small basins. In addition, CHIRPS was found to be as  
126 accurate as or even better than other seven commonly used precipitation products in Adige Basin  
127 in Italy after comprehensive evaluation at multiple temporal (daily to annual) and spatial scales  
128 (Duan et al., 2016). The follow-up study further demonstrated that using the CHIRPS product as  
129 input to the SWAT model resulted in satisfactory performance in simulating monthly streamflow  
130 in the same basin (Tuo et al., 2016). A recent evaluation showed that the CHIRPS precipitation  
131 data have higher accuracy than other four gridded precipitation datasets in the Upper Blue Nile  
132 Basin (Bayissa et al., 2017). The evaluation was carried out by comparing gridded dataset with  
133 gauge-based measurements at daily, monthly, and seasonal time scales. Given its aforementioned  
134 special feature and good performance, CHIRPS can be a good alternative open-access data  
135 source in various applications. To our best knowledge, no study has been conducted to evaluate  
136 the performance of using CHIRPS precipitation in driving SWAT to simulate streamflow at the  
137 daily scale.

138 In this study, we focused on a basin upper Gilgel Abay within Lake Tana Basin in Ethiopia  
139 where the data scarcity has been mentioned in many previous studies. The data scarcity motives  
140 us to explore the alternative data source particularly the relatively new CHIRPS precipitation  
141 data. The main objective of this study is to determine the suitable weather data inputs for SWAT  
142 in this data-scarce basin. We evaluated the performance of using different combinations of four  
143 precipitation datasets (gauge and three open-access datasets, CHIRPS, TRMM, CFSR) and two  
144 air temperature datasets (gauge and CFSR) in driving SWAT for daily and monthly streamflow  
145 simulation.

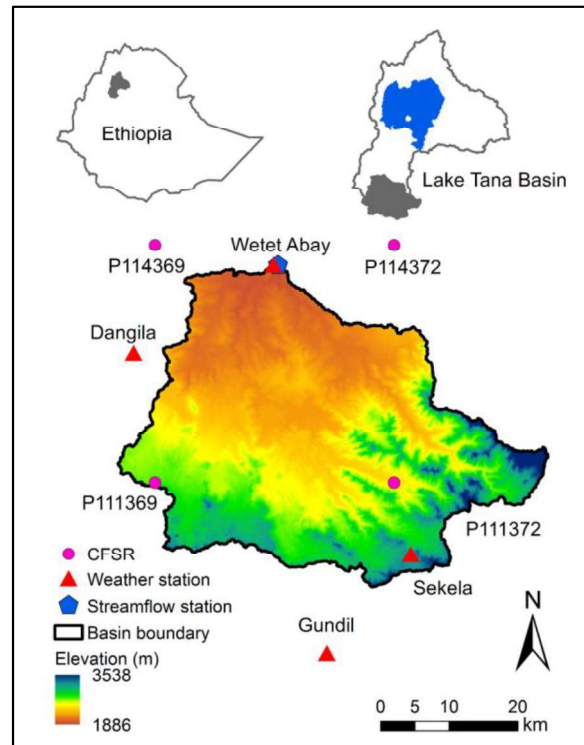
146 The remainder of this paper is organized as follows: Section 2 introduces the study area. Section  
147 3 provides a brief description of data and methods. Section 4 presents the detailed results and  
148 discussion. Finally, Section 5 summarizes main findings and additional suggestion for future  
149 studies.

## 150 **2 Study area**

151 The upper Gilgel Abay Basin is located in northwestern highlands of Ethiopia (Fig. 1) It belongs  
152 to the Lake Tana Basin. Lake Tana is the largest lake in Ethiopia and the third largest in the Nile  
153 River Basin (Setegn et al., 2010). Lake Tana is a vast circular-shaped and shallow lake with  
154 water level fluctuations of approximately 1.6 m among seasons. The surface water area of Lake  
155 Tana ranges from 2966 to around 3100 km<sup>2</sup> depending on the seasonal fluctuation of lake level  
156 (Duan & Bastiaanssen, 2013b). Lake Tana is the source of the Blue Nile River and the Blue Nile  
157 River contributes more than 60% of total flow into the Nile River at Aswan in Egypt  
158 (Uhlenbrook et al., 2010). Therefore, water resources of Lake Tana are of great importance for  
159 Ethiopia and other Nile Basin riparian countries. Despite of such importance, Lake Tana Basin is



160 a poorly gauged basin with ungauged areas accounting for more than 50% of the total area (Wale  
161 et al., 2009). Previous studies showed that more than 93% of lake inflow is from four main  
162 tributary rivers and the Gilgel Abay is the main tributary by contributing about 60% of the inflow  
163 to the lake (Uhlenbrook et al., 2010).



164

165 **Fig. 1.** Locations of the upper Gilgel Abay Basin, one streamflow gauging station and four  
166 weather stations, and CFSR stations.

167 The upper Gilgel Abay Basin has a total area of 1656 km<sup>2</sup>. The elevation ranges from 1886 to  
168 3538 m above the mean sea level. The high elevation is located in the southern, west and  
169 southeast part. The geology is composed of quaternary basalts and alluviums and the dominant  
170 land use types are agricultural and agro-pastoral land with rainfed agriculture accounting for 74%  
171 (Uhlenbrook et al., 2010). The dominant soil type is clay. The mean annual precipitation is 1811

172 mm/year based on the analysis of available rain gauge data between 2000 and 2007. The climate  
173 of this region is tropical highland monsoon with a rainy season (June–September) and a dry  
174 season (October–March). The seasonal distribution of rainfall is mainly controlled by the north–  
175 south movement of the Inter Tropical Convergence Zone (ITCZ) (Taye & Willems, 2012). The  
176 air temperature shows a large diurnal but small seasonal variability. Based on measured air  
177 temperature from gauge stations for the period 2000-2007, the annual mean daily maximum air  
178 temperature is 25.4°C and minimum air temperature is 9.8°C, and the daily average air  
179 temperature is 17.6°C.

### 180 **3 Datasets and methods**

#### 181 3.1 In-situ measurements from gauge stations

182 In-situ measurements of weather data from four gauge stations were obtained from Ethiopian  
183 National Meteorological Agency. Measured daily streamflow from a single station at the outlet  
184 of upper Gilgel Abay Basin were obtained from the Hydrology Department of the Ministry of  
185 Water Resources of Ethiopia. The locations of these stations are shown in Fig. 1. For weather  
186 data, two stations (Wetet Abay and Sekela) are within the basin and the other two (Dangila and  
187 Gundil) are around with Dangila station being much closer to the basin. After intensive and  
188 rigorous analyses of measured data, finally the available data constrained us to focus on the  
189 period 1998-2007 for which data are relatively more complete. For this period, all four stations  
190 had daily precipitation data, while three stations excluding Sekela had daily maximum and  
191 minimum air temperature, but there were still temporal gaps with more substantial for air  
192 temperature data than precipitation. The data gaps and scarcity in this region have been  
193 commonly mentioned in many previous studies (Dile & Srinivasan, 2014; Roth & Lemann,

194 2016), which is indeed the motivation of this study for exploring the performance of alternative  
195 open-access weather data. Fig. 2 shows the summary of data gaps for precipitation and air  
196 temperature. It is worth noting that in some period, data were available in only one station. For  
197 example, from October to December in 2002, daily maximum temperature was only available in  
198 the Wetet Abay station. Considerable uncertainty existed in such situations. The SWAT model  
199 can automatically fill missing weather data by using weather generator which needs more efforts  
200 and more historical data to prepare. In this study, we filled the data gaps before using them as  
201 inputs to SWAT. The data gaps were filled as follows: for the dates of data gaps, the data from  
202 the closest station were used if possible. In the case of all stations have data gaps for certain  
203 dates, then the data gaps were filled by taking available data from the same dates in the closest  
204 years for the same station. In this study, we did not interpolate weather stations data as there  
205 were only four stations that are insufficient for a reasonable interpolation based on geostatistical  
206 methods. We used the weather stations in the normal/standard way to SWAT. The SWAT model  
207 (ArcSWAT interface) will automatically distribute the weather data to the subbasins by using  
208 data from only one gauge station that is nearest to the centroid of each subbasin (Tuo et al.,  
209 2016).

1998	365	365	365	4	39	34	7	0	0	4
1999	365	365	184	9	0	0	12	0	0	0
2000	337	366	4	18	0	0	35	1	1	5
2001	0	140	10	7	0	0	7	26	0	3
2002	1	121	1	7	103	0	31	295	0	0
2003	0	0	0	6	0	0	8	29	0	1
2004	13	13	0	30	0	0	8	0	0	1
2005	0	0	0	48	31	32	8	212	212	215
2006	31	31	0	0	0	0	1	31	31	44
2007	39	39	8	55	1	2	2	0	0	5
	Wetet Abay-TMX	Wetet Abay-TMN	Wetet Abay-P	Sekela-P	Dangjila-TMX	Dangjila-TMN	Dangjila-P	Gundil-TMX	Gundil-TMN	Gundil-P

210

211 **Fig. 2.** Data gaps for air temperature and precipitation gauge data. The number in each grid  
 212 means the number of days with missing data in each year. TMX, TMN, P means daily maximum  
 213 temperature, minimum temperature and precipitation, respectively.

214 For streamflow data, the station had more complete data with only 19 values missing (October 8-  
 215 26, 2006) during the entire period. Streamflow data were used for calibration and validation of  
 216 the SWAT model in streamflow simulation. The 19 missing data were within the validation  
 217 period, in this study they were not filled and instead these dates with missing data (October 2006)  
 218 were simply discarded for validation to avoid additional uncertainty caused by gap-filling.

### 219 3.2 CHIRPS precipitation data

220 CHIRPS stands for the Climate Hazards Group InfraRed Precipitation with Station data. The  
221 CHIRPS data provides daily precipitation data at the spatial resolution of  $0.05^\circ$  for the quasi-  
222 global coverage of  $50^\circ\text{N}$ - $50^\circ\text{S}$  from 1981 to present. The latest product is the Version 2.0  
223 product that was released in February 2015. The CHIRPS product and its supporting data are  
224 available at: <http://chg.geog.ucsb.edu/data/chirps/>. The main used datasets for the construction of  
225 CHIRPS product include the monthly precipitation climatology (CHPclim) that is created using  
226 rain gauge stations collected from FAO and GHCN, the Cold Cloud Duration (CCD) information  
227 based on thermal infrared data archived from CPC and NOAA National Climate Data Center  
228 (NCDC), the Version 7 TRMM 3B42 data, the Version 2 atmospheric model rainfall field from  
229 the NOAA Climate Forecast System (CFS), and the rain gauge stations data from multiple  
230 sources. First, the CCD data are calibrated with TRMM 3B42 to generate the 5-daily CCD-based  
231 precipitation estimates which are further converted to the fractions of the long-term mean  
232 precipitation estimates. The fractions are then multiplied with CHPclim data to remove the  
233 systematic bias and the derived product is called CHIRP product. Finally, the CHIRP product is  
234 blended with rain gauge stations data using a modified inverse distance weighting algorithm to  
235 produce the CHIRPS. All the processing mentioned above are performed at the 5-daily  
236 timescales. The daily CCD data and daily CFS data are finally used to disaggregate the 5-daily  
237 products to daily precipitation estimates using a simple redistribution method. More detailed  
238 information on CHIRPS can be found in Funk et al. (2015). Daily CHIRPS products at the  
239 spatial resolution of  $0.05^\circ$  the period 1998-2007 were used and evaluated in this study. SWAT  
240 does not allow to directly use gridded precipitation as input as it is not a fully distributed model.  
241 Thus we computed the area-weighted average daily CHIRPS data from all grids within the

242 subbasin to represent the effective daily precipitation for each subbasin and then further using  
243 them as input to the SWAT model following Tuo et al. (2016). To avoid the edge effect during  
244 averaging, the CHIRPS grid cells were firstly disaggregated by 10 times ( $0.005^\circ$ ) but  
245 maintaining original grid locations and values before performing area-weighted averaging.

### 246 3.3 TRMM 3B42 precipitation data

247 The TRMM 3B42 product is one type of the TMPA (TRMM Multi-satellite Precipitation  
248 Analysis) products (Huffman et al., 2007). TRMM 3B42 product provides 3-hourly and daily  
249 precipitation at the spatial resolution of  $0.25^\circ$  for the quasi-global coverage of  $50^\circ$  N– $50^\circ$  S from  
250 1998 to present. The applied algorithm is the TMPA algorithm that combines precipitation  
251 estimates from microwave and infrared satellites, as well as the gauge-interpolated monthly  
252 gridded product from GPCC (Global Precipitation Climatology Centre). More details about  
253 TMPA algorithms can be found in (Huffman et al., 2007) and Huffman and Bolvin (2015). All  
254 TRMM products including 3B42 can be freely downloaded from Goddard Earth Sciences Data  
255 and Information Services Center at <http://mirador.gsfc.nasa.gov> and other sources. The latest  
256 version (Version 7) daily accumulated TRMM 3B42 product for the common period 1998-2007  
257 were used in this study, and the data are simply referred to TRMM for conciseness hereafter.  
258 Similarly, we firstly disaggregated the TRMM grids by 50 times (to  $0.005^\circ$ ) to reduce the edge  
259 effect during averaging. Then area-weighted average daily TRMM data from all grids within the  
260 subbasin were computed to represent the effective daily precipitation for each subbasin, which  
261 were then used as inputs of the SWAT model.

### 262 3.4 CFSR precipitation and air temperature data

263 The CFSR, as the product of the National Centers for Environmental Prediction (NCEP), was  
264 designed and executed as a global coupled atmosphere–ocean–land surface–sea ice system to  
265 provide the best estimate of the state of these coupled domains (Saha et al., 2010). This system  
266 uses most available in situ and satellite observations and provides a range of atmospheric,  
267 oceanic, and land surface output products at an hourly time resolution for any geographic  
268 location around the globe. The CFSR global atmosphere products are at the spatial resolution of  
269 ~38 km with 64 levels extending from the surface to 0.26 hPa. More details about CFSR can be  
270 found in Saha et al. (2010). The available CFSR data spans from 1979 to 2014 with planned  
271 update to present. The online Global Weather Data for SWAT data portal  
272 <https://globalweather.tamu.edu/> popularizes the application of CFSR in SWAT modelling  
273 community because it provides readily weather data (precipitation, air temperature, relative  
274 humidity, wind speed and solar radiation) required by SWAT in the ready-to-use format.  
275 Specially, this data portal provides CFSR data like a normal weather station using the centroid of  
276 the CFSR grid as the coordinate of each CFSR weather point/station (Dile and Srinivasan, 2014).  
277 Users just need to enter the coordinates of the bounding box covering the area of interest and  
278 then the data portal would generate the required weather data from the CFSR weather stations  
279 within the box. We followed the norm to request the precipitation and air temperature data  
280 covering the upper Gilgel Abay Basin for the period 1998-2007 and they were directly used as  
281 inputs to the SWAT model. The locations of CFSR weather stations are shown in Fig. 1. Finally  
282 only three CFSR weather stations (P114369, P111369 and P111372) located in or closer to the  
283 Gilgel Abay Basin were actually used in the SWAT model as the SWAT model automatically  
284 selects only one gauge station that is nearest to the centroid of each subbasin (Tuo et al., 2016).

### 285 3.5 SWAT model and model setup

286 SWAT stands for Soil and Water Assessment Tool. It is a semi-distributed, process-based and  
287 time-continuous river basin model, which was developed by the Agricultural Research Service of  
288 the United States Department of Agriculture-Agricultural Research Service (Arnold et al., 1998).  
289 SWAT can be used to model hydrological processes, soil erosion, and water quality in river  
290 basins and evaluate the impact of land use change/land management practices on water, sediment  
291 and nutrients yields (Neitsch et al., 2011; Song et al., 2011; Tuo et al., 2016). In SWAT, the river  
292 basin is first divided to subbasins and further to the Hydrologic Response Units (HRUs) which is  
293 the smallest spatial unit. The HRU is generated by a unique combination of land use, soil type  
294 and slope. Simulation of hydrology consists of two major phases: the land phase and routing  
295 phase. For the land phase, the hydrological cycle simulated by SWAT is based on the soil water  
296 balance, and this phase calculates the quantity of water, sediment and nutrients loads from land  
297 to the main channel. SWAT offers two methods for estimating surface runoff: the SCS curve  
298 number method (USDA-SCS, 1972) that requires daily precipitation as input and the Green and  
299 Ampt infiltration method (Green & Ampt, 1911) that requires sub-daily precipitation. The  
300 routing phase controls the movement of these loads through the channel network to the outlet of  
301 a river basin. The Manning's equation is used to define the rate and velocity of channel flow and  
302 flow/water is routed through channels using either variable storage routing or Muskingum  
303 routing. More details about the SWAT model can be found in the official theoretical  
304 documentation (Neitsch et al., 2011) and review paper (Gassman et al., 2007) as well as SWAT  
305 literature database available at [https://www.card.iastate.edu/swat\\_articles/](https://www.card.iastate.edu/swat_articles/). The SWAT model  
306 has been embedded as easy-to-use toolbar as ArcSWAT in ArcGIS interface. The ArcSWAT  
307 (Version 2012.10\_3.18) was used for setting up SWAT model in this study.



308 Besides the weather data, which the detailed procedures are mentioned above, the SWAT model  
309 requires elevation data, land use map and soil map with information on soil properties. Below  
310 describes the data source and processing for setting up the SWAT model in our study. The  
311 Digital Elevation Model (DEM) data at the spatial resolution of about 30 m from the Shuttle  
312 Radar Topographic Mission 1 arc-second global product were downloaded from USGS  
313 EarthExplorer at <https://earthexplorer.usgs.gov/>. The DEM was used to perform the automatic  
314 watershed delineation and used to compute topographic parameters for the SWAT model. The  
315 land use map representing the year of 2004 was obtained from the International Livestock  
316 Research Institute (ILRI) at <http://data.ilri.org/geoportal/catalog/main/home.page>. The world soil  
317 map developed by the Food and Agriculture Organization (FAO) at 1:5000000 scale was  
318 obtained at [http://www.fao.org/soils-portal/soil-survey/soil-maps-and-databases/faunesco-soil-  
319 map-of-the-world/en/](http://www.fao.org/soils-portal/soil-survey/soil-maps-and-databases/faunesco-soil-map-of-the-world/en/). Similar to Mekonnen et al. (2018), the Harmonized World Soil Database  
320 v1.2 together with this FAO soil map and associated information was used to prepare the  
321 required soil properties in SWAT.

322 SWAT also provides several options for calculating certain hydrological components such as  
323 potential evapotranspiration. The default setting for potential evapotranspiration is the Penman–  
324 Monteith method which requires more weather data (i.e., wind speed and solar radiation and  
325 relative humidity) than the simple Hargreaves method (Hargreaves & Samani, 1982) which  
326 requires only air temperature data. Given the common data scarcity, like most previous studies in  
327 this study area or nearby regions (Dile & Srinivasan, 2014; Setegn et al., 2010; Tekleab et al.,  
328 2011), we used the Hargreaves method for calculating potential evapotranspiration in this study,  
329 and all other default settings (e.g. the SCS curve number method for surface runoff and the  
330 variable storage routing method for water routing) in SWAT were used.

331 By only changing different weather data (precipitation and air temperature) as inputs, we were  
332 able to set up a number of eight model scenarios, a combination of two air temperature data  
333 (guage and CFSR) and four precipitation data (guage, CHIRPS, TRMM, and CFSR), to  
334 investigate the effects of different weather data on streamflow simulation.

### 335 3.6 Model calibration using SWAT-CUP and model evaluation

336 In this study, for all eight model scenarios, the SWAT model was run at daily timescale, and the  
337 first two years (1998-1999) were considered as warm-up period to mitigate the effect of initial  
338 conditions of hydrological modelling. The period 2000-2003 was considered as calibration  
339 period, in which sensitivity parameters were calibrated to fit the observed daily streamflow. The  
340 remaining period 2004-2007 was used for validation.

341 The automatic calibration was performed for daily streamflow simulation by using the Sequential  
342 Uncertainty Fitting algorithm version 2 (SUFI-2) (Abbaspour et al., 2004; Abbaspour et al., 2007)  
343 in the SWAT-CUP tool (Abbaspour, 2015). The sensitivity analysis was firstly performed with  
344 SWAT-CUP using one-at-a-time procedure (Abbaspour, 2015) and a number of eight parameters  
345 were finally identified as highly sensitive parameters (Table 1). The selection of sensitive  
346 parameters is consistent with previous studies (Mekonnen et al., 2018; Setegn et al., 2010). In  
347 this study, the same eight parameters were considered for calibration for each SWAT model. The  
348 same initial range (Table 1) was used for the eight parameters among all SWAT models to  
349 enable a fair starting point and comparison. Following Abbaspour (2015), the calibration  
350 procedures were performed with three iterations with 1000 simulations (so a total 3000  
351 simulations during the calibration) being run for each iteration using the Nash-Sutcliffe  
352 Efficiency (NSE, Nash & Sutcliffe, 1970) as the objective function. After each iteration, the

353 range of each parameter was updated (normally narrowed down) based on both the new  
354 parameters suggested by the SWAT-CUP tool (Abbaspour et al., 2004; Abbaspour et al., 2007)  
355 and their reasonable physical boundaries. More details about the calibration procedures can be  
356 found in Abbaspour (2015) and Abbaspour et al. (2015). For evaluating model performance in  
357 streamflow simulation using different precipitation and air temperature as inputs, the best one  
358 among the 3000 simulations from each SWAT model was compared.

359 For model evaluation and comparison purpose, we used three indicators, i.e. NSE and the  
360 coefficient of determination ( $R^2$ ) and the percent bias (PBIAS, %). Calculations of these  
361 indicators were performed using R package hydroGOF (Zambrano-Bigiarini, M., 2014). The  
362 NSE measures the quantity difference between the simulated streamflow and the measured  
363 streamflow, a value of 1 is the optimal value for NSE, a negative value of NSE means that the  
364 model has no skill in the simulation compared to simply using the mean as a predictor (Bitew &  
365 Gebremichael, 2011). The  $R^2$  ranges from 0 to 1 and represents the trend similarity between the  
366 simulated streamflow and measured. The closer the  $R^2$  value to the optimal value of 1, the better  
367 model performance is. The PBIAS measures the average tendency of the simulated values to be  
368 larger or smaller than the corresponding observed values. The optimal PBIAS value is 0, and  
369 positive (negative) values indicate overestimation (underestimation) bias in the simulation. We  
370 followed the criteria proposed by Moriasi et al. (2007) to classify the performance of model to  
371 the respective categories: unsatisfactory ( $NSE \leq 0.50$ ,  $PBIAS \geq \pm 25\%$ ), satisfactory  
372 ( $0.50 < NSE \leq 0.65$ ,  $\pm 15\% \leq PBIAS < \pm 25\%$ ), good ( $0.65 < NSE \leq 0.75$ ;  $\pm 10\% \leq PBIAS < \pm 15\%$ ) and  
373 very good ( $NSE > 0.75$ ,  $PBIAS < \pm 10\%$ ).

374

375 **Table 1**

376 List of eight parameters considered for calibration and their default values, calibrated ranges and  
 377 physical ranges. In the SWAT-CUP “a\_\_”, “v\_\_” and “r\_\_” means to modify the default  
 378 value by adding a specified value, to replace the default value by the specified value, and to  
 379 make a relative change to the initial parameter values, respectively (Abbaspour, 2015). More  
 380 details on parameter calibration with SWAT-CUP can be found in Yang et al. (2008) and Tuo et  
 381 al., (2016).

Parameters	Description	Default	Calibrated range	Physical range
r_CN2.mgt	SCS runoff curve number	HRU specific	-0.3/0.1	35/98
r_SOL_AWC.sol	Available water capacity of the soil layer[mm H <sub>2</sub> O/mm soil]	Soil layer specific	-0.5/0.5	0/1
v_ESCO.hru	Soil evaporation compensation factor	0.95	0/1	0/1
v_GW_DELAY.gw	Groundwater delay [days]	31	0/500	0/500
v_GW_REVAP.gw	Groundwater "revap" coefficient	0.02	0.02/0.2	0.02/1
v_GWQMN.gw	Threshold depth of water in the shallow aquifer required for return flow to occur [mm]	1000	0/5000	0/5000
a_REVAPMN.gw	Threshold depth of water in the shallow aquifer for "revap" to occur [mm]	750	-500/250	0/1000
v_CH_K2.rte	Effective hydraulic conductivity [mm/hr]	0	0/150	-0.01/500

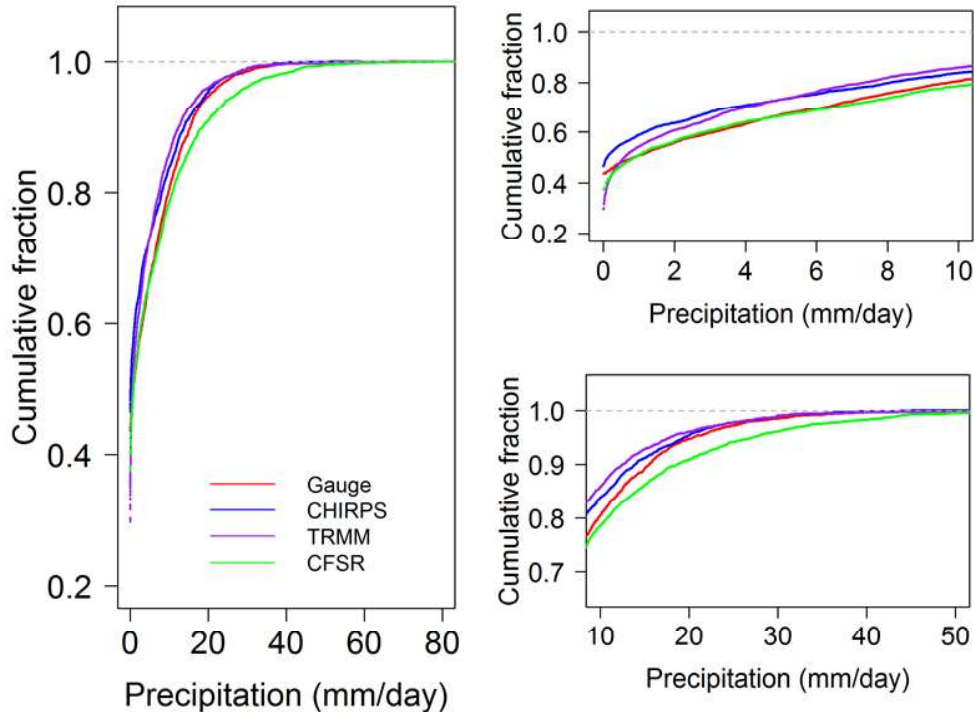
382

383 **4 Results and discussion**

384 4.1 Comparison of precipitation and temperature inputs

385 Fig. 3 shows the cumulative fraction of the daily precipitation averaged over the studied basin  
 386 from four sources during the calibration and validation period (2000-2007). Four products  
 387 display different probability of occurrence of dry day (rain=0 mm/day), which are 44%, 47%, 30%

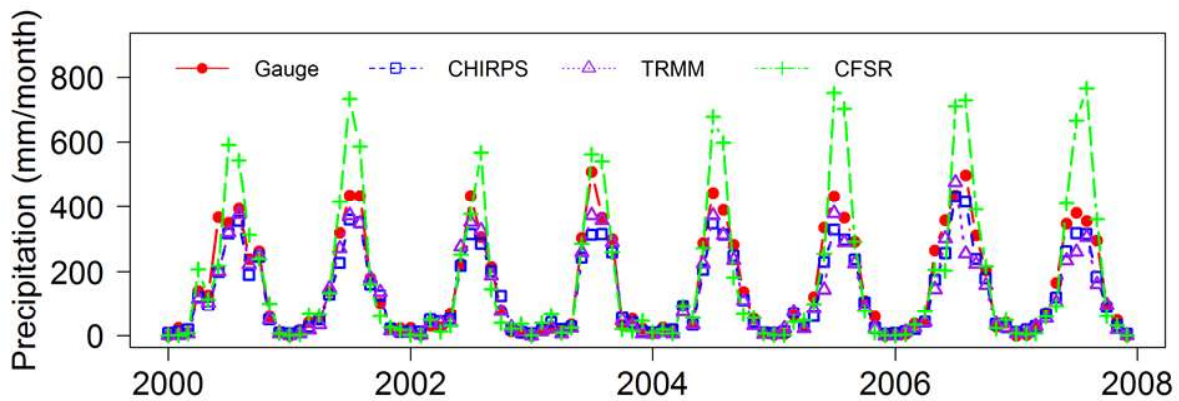
388 and 38% for gauge, CHIRPS, TRMM and CFSR, respectively. Overall all, CHIRPS and TRMM  
 389 had very similar distribution for all precipitation intensity expect for the dry days. The difference  
 390 in dry days between CHIRPS and TRMM could be partly due to the spatial resolution issue;  
 391 TRMM spreads the rain out over the 0.25° pixels that may contain 0.05° pixels with no rain as  
 392 indicated by CHIRPS. For precipitation intensity with 0-10 mm/day, the distribution of CFSR is  
 393 very close to that of the gauge measurements. Four products showed larger difference for  
 394 precipitation within 10-50 mm /day within largest being at the threshold of 20 mm/day. The  
 395 CFSR data set had the highest frequency (10%) of precipitation beyond 20 mm/day, while the  
 396 other three data sets had less than 5%. The average annual precipitation from 2000 to 2007 were  
 397 1811 mm, 1491 mm, 1471 mm and 2173 mm for gauge, CHIRPS, TRMM and CFSR,  
 398 respectively.



399

400 **Fig. 3.**The cumulative fraction of daily precipitation from four data sets (Gauge, CHIRPS,  
401 TRMM and CFSR) at the basin scale during 2000-2007.

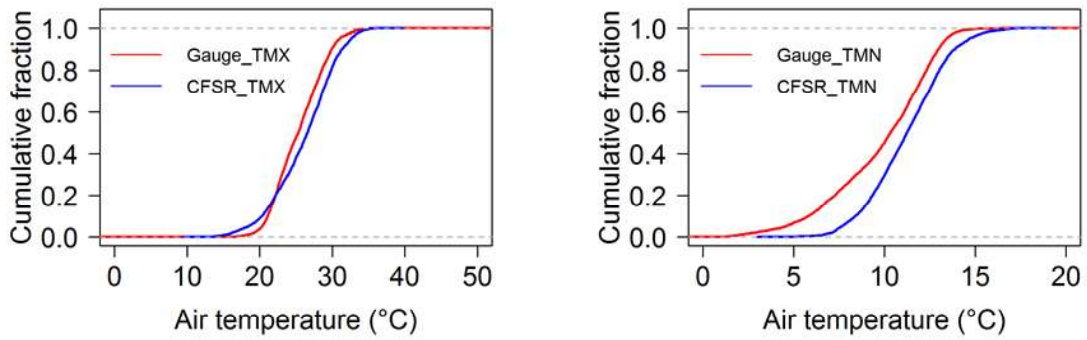
402 Fig. 4 shows the comparison of monthly precipitation over the basin from four datasets. All four  
403 datasets showed the same seasonal pattern with rainy months centered in June-September.  
404 However, clearly CFSR consistently had more precipitation than the other three data sets for the  
405 rainy months through the entire period, especially during the validation period (2004-2007). The  
406 pattern and magnitude of monthly precipitation from CHIRPS and TRMM data set were much  
407 similar. Both data sets were in much better agreement with gauged precipitation through the  
408 entire period, but their peaks were usually lower than gauge data.



410 **Fig. 4.** Comparison of monthly precipitation totals from four data sets (gauge, CHIRPS, TRMM  
411 and CFSR) at the basin scale during 2000-2007.

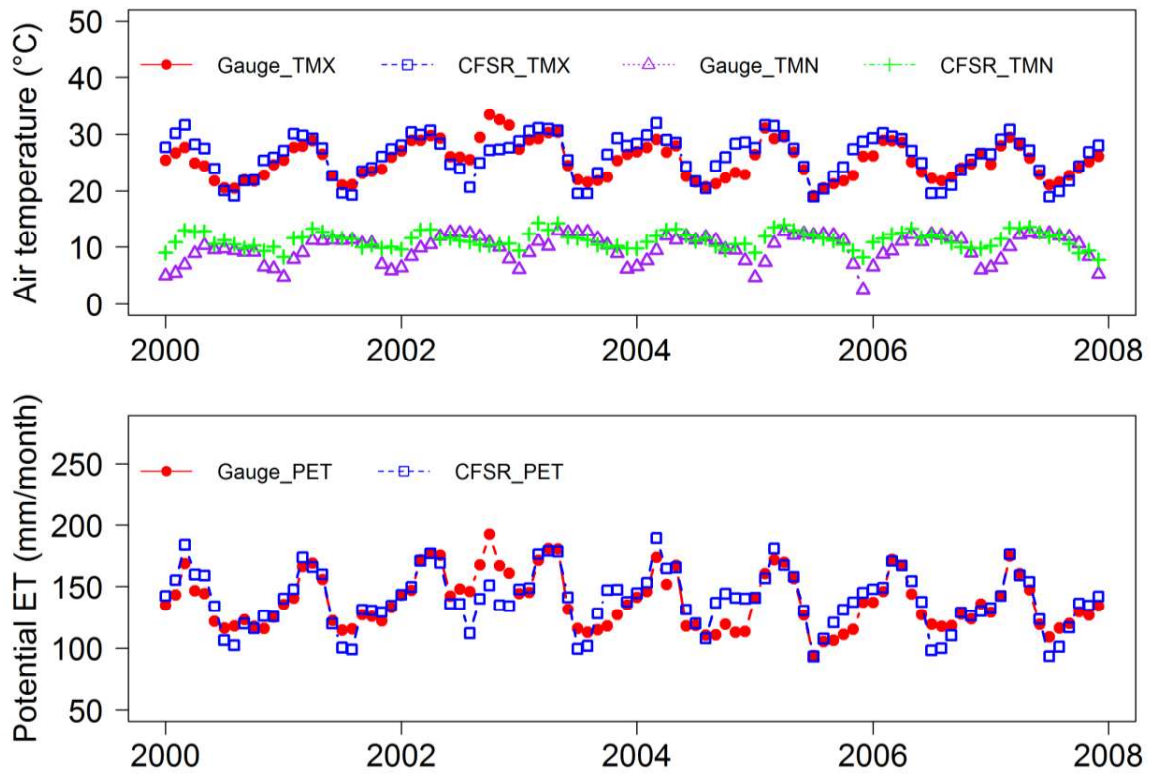
412 Fig. 5 displays the cumulative fraction of daily maximum and minimum air temperature at the  
413 basin scale from the two data sets (gauge and CFSR) during 2000-2007. Fig. 6 presents the  
414 monthly mean of daily maximum and minimum air temperature. Overall, CFSR data set agreed  
415 better with gauge measurements for the daily maximum air temperature than for the daily

416 minimum air temperature. Similar finding was reported in two basins in Malaysia (Tan et al.,  
417 2017). For the daily maximum air temperature, two data sets showed good similarity in the  
418 seasonal pattern and magnitude during the entire period except for four months in 2002 when  
419 daily maximum temperature was only available in the Wetet Abay station. Analysis of historical  
420 air temperature data showed that Wetet Abay station had higher daily maximum air temperature  
421 than other stations. Therefore, using gauge data from only Wetet Abay station biased toward  
422 higher average daily maximum air temperature at the basin scale in 2002 (Figure 6).  
423 There is no snowfall in this study area and thus the air temperature input would be mainly used  
424 to compute the potential evapotranspiration (PET) in SWAT. The resulting PET would further  
425 affect the computation of water balance in SWAT. To explore the impact of using air  
426 temperature input from the two data sets on SWAT modelling, we further compared the PET  
427 estimates. The time-series of monthly PET totals from the two data sets are shown in Fig. 6. The  
428 seasonal pattern of PET is very similar to that of daily maximum air temperature. Similarly, the  
429 PET estimates from two data sets were in good agreement except for the same periods when  
430 larger discrepancy occurred in daily maximum air temperature. Therefore, given such good  
431 agreement in PET estimates, we expected the impacts of using air temperature input from the  
432 two data sets would have very limited influence on the SWAT modelling results, which was  
433 ascertained in our following analysis.



434

435 **Fig. 5.** The cumulative fraction of daily maximum (TMX) and minimum (TMN) air temperature  
 436 from gauge and CFSR data set at the basin scale during 2000-2007.



437

438 **Fig. 6.** Comparison of monthly mean daily maximum (TMX) and minimum (TMN) air  
 439 temperature from gauge and CFSR data set, and their resulting potential evapotranspiration (PET)  
 440 estimates at the basin scale during 2000-2007.



## 441 4.2 Results of streamflow simulation using different precipitation and temperature inputs

### 442 4.2.1 Simulation results without calibration

443 We first evaluated the performance of all eight models without calibration. For conciseness,  
444 hydrographs of results without calibration are not shown here, but the model evaluation statistics  
445 at the daily and monthly timescales are presented in Table 2 and 3, respectively. According to the  
446 guidelines by Moriasi et al. (2007), all eight model scenarios yielded unsatisfactory daily  
447 streamflow simulation with NSE values of less than 0.5 for both two periods 2000-2003 and  
448 2004-2007. Only the two models with gauge precipitation input had PBIAS less than 10%,  
449 indicating the very good performance on average. The models using the same precipitation but  
450 different air temperature inputs had almost the same performance. Using CFSR precipitation as  
451 input resulted in the worst performance with lowest NSE values of 0.05 and -1.1 and high  
452 positive PBAIS values of around 19% and over 46% for the two considered periods, respectively.  
453 This is mainly due to the high overestimation in precipitation by CFSR (Fig. 3). As far as the  
454 performance at the monthly scale is concerned, almost all eight models yielded quite good  
455 monthly streamflow simulation with  $NSE > 0.64$  and  $R^2 > 0.82$  (except for the period 2004-2007  
456 using CFSR precipitation data). All models except ones with gauge precipitation input had high  
457 PBIAS values showing the average tendency of considerable underestimation in simulations by  
458 using CHIRPS and TRMM as inputs or overestimation in simulations by using CFSR as input.  
459 Using gauge precipitation as input performed best with both NSE and  $R^2$  values larger than 0.90  
460 and small PBIAS. Models using precipitation from CHIRPS and TRMM performed comparably  
461 with TRMM slightly better for 2000-2003 while CHIRPS better for 2004-2007. During 2000-  
462 2003, using CFSR precipitation as input even outperformed CHIRPS and TRMM, but it yield

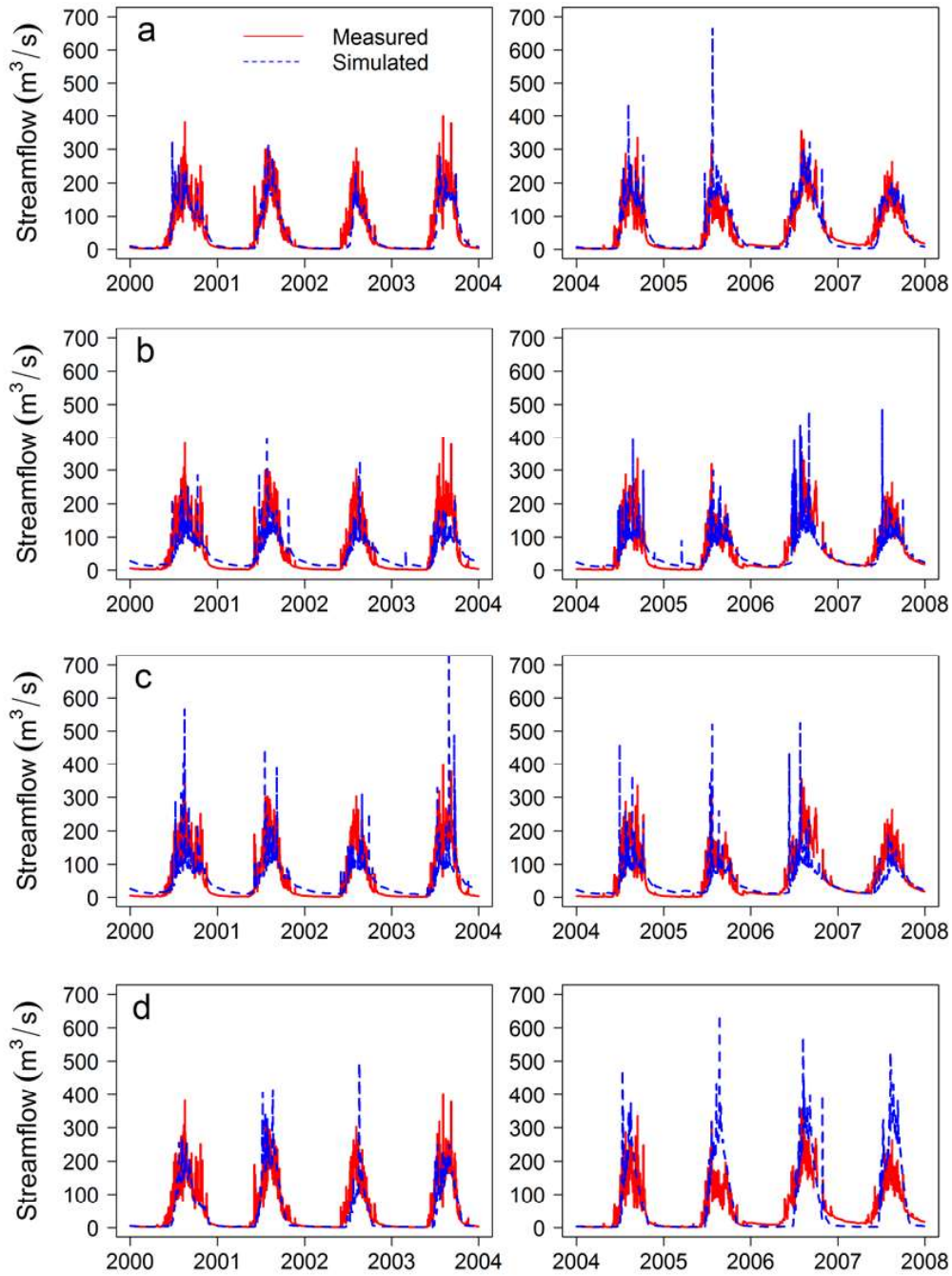
463 unsatisfactory simulation (significant overestimation in streamflow) for 2004-2007 with NSE of  
464 0.07.

#### 465 4.2.2 Simulation results after calibration

466 Fig. 7 shows comparison of daily measured and simulated streamflow from the four models  
467 using gauge air temperature and four different precipitation data sets for the calibration (2000-  
468 2003) and validation (2004-2007) periods after calibration. Fig. 8 shows the same as Fig. 7  
469 except using CFSF air temperature as input instead of gauge data. Fig. 9 and 10 shows  
470 simulation results at the monthly scale for all eight models. Table 2 and 3 summarizes model  
471 evaluation statistics for all eight models at the daily and monthly timescales, respectively. It can  
472 be found that if the same precipitation dataset was used, using gauge and CFSR air temperature  
473 datasets had almost identical performance.

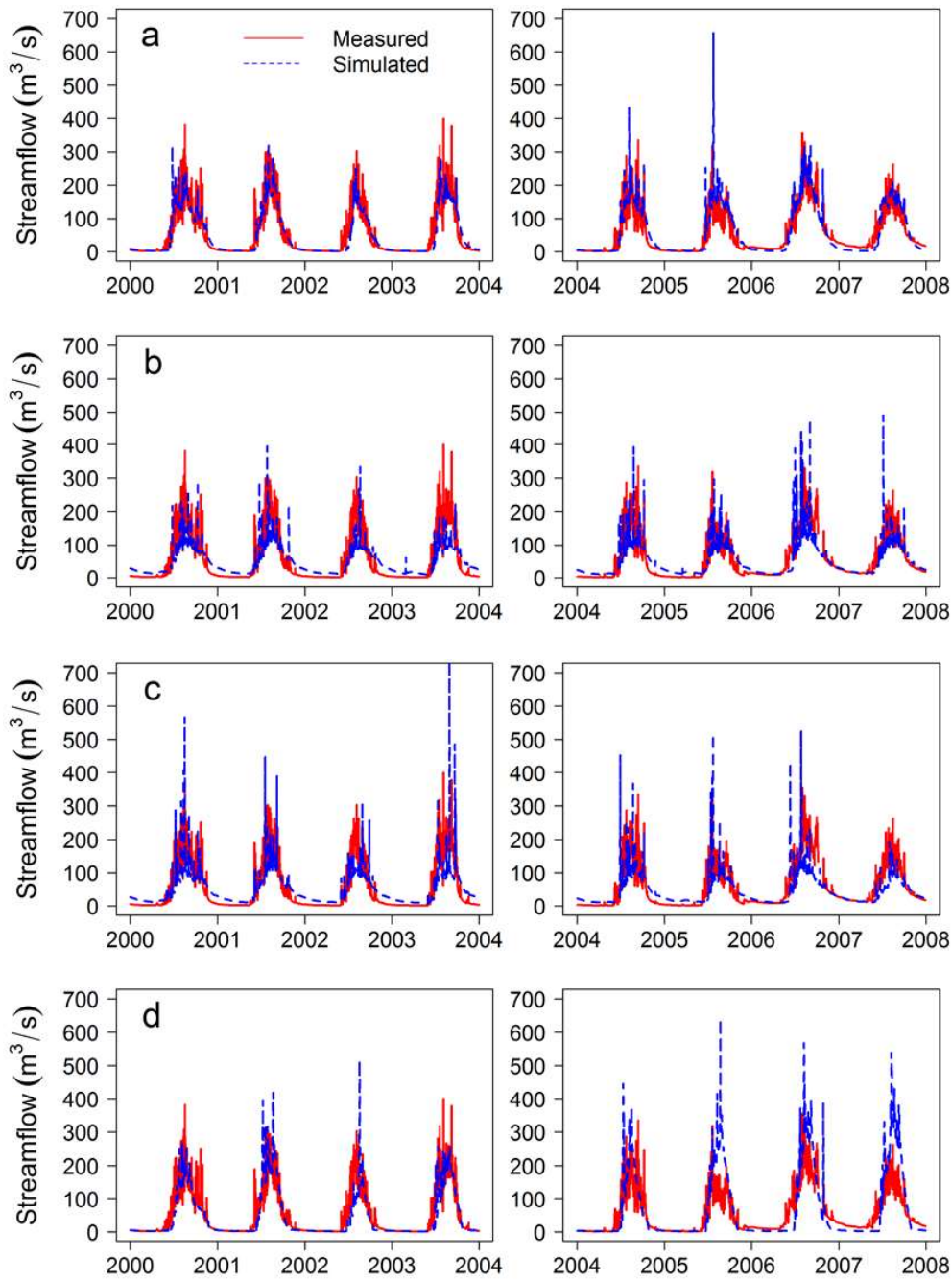
474 Overall most models can well captured seasonal patterns. Hydrograph at the daily timescale (Fig.  
475 7 and Fig. 8) showed reasonable agreement between the observed and simulated streamflow  
476 using gauge and CHIRPS precipitation as inputs except overestimation and underestimation in a  
477 very few events. Using gauge precipitation performed best in daily streamflow simulation with  
478 NSE of 0.69 to 0.78. This translates into very good and good performance according to the  
479 guideline by Moriasi et al. (2007). The noticeable overestimation in 25 July 2005 during the  
480 validation period was caused by the recorded extremely high precipitation from Sekela station  
481 (103.5 mm/day). Using CHIRPS precipitation yielded satisfactory performance with NSE of 0.52  
482 to 0.57 and very good performance in terms of PBIAS within 10%. Using TRMM precipitation  
483 yielded unsatisfactory performance in terms of NSE, but the NSE were very close to the  
484 threshold 0.50 of being satisfactory, and PBIAS within 25% shows satisfactory performance on

485 average simulations. Using CFSR precipitation resulted in satisfactory performance which was  
486 even slightly better than that using gauge precipitation for the calibration period, but the  
487 performance was very poor for the independent validation period with NSE of 0.01/0.04. This  
488 suggests that the calibrated parameters cannot be used for prediction, which is mainly due to the  
489 inconsistent behavior of CFSR precipitation in the two periods. As shown in Fig. 7 and Fig. 8,  
490 the overestimation of precipitation by CFSR appears to be more severe during the validation  
491 period than during the calibration period, and thus the calibrated parameters cannot compensate  
492 for such overestimation.



493

494 **Fig. 7.** Comparison of daily measured and simulated streamflow from models using gauge air  
 495 temperature and four different precipitation datasets (a: Gauge, b: CHIRPS, c: TRMM, d: CFSR)  
 496 for the calibration period 2000-2003 and validation period 2004-2007.



497

498 **Fig. 8.** Comparison of daily measured and simulated streamflow from models using CFSR air  
 499 temperature and four different precipitation datasets (a: Gauge, b: CHIRPS, c: TRMM, d: CFSR)  
 500 for the calibration period 2000-2003 and validation period 2004-2007.

501 When daily results were aggregated to monthly timescale, all models showed better performance  
502 with good agreement with measured streamflow in hydrography (Fig. 9 and Fig. 10) and better  
503 evaluation statistics (Table 3). Using gauge precipitation still yielded better performance than the  
504 other three precipitation datasets with NSE of 0.92 for both calibration and validation period.  
505 CHIRPS and TRMM performed comparably well with each being better for a certain period, but  
506 hydrography showed both overestimated low flow and underestimate high flow through the  
507 entire period 2000-2007. Using CFSR precipitation still cannot satisfactorily simulate monthly  
508 streamflow during the validation period with NSE of 0.26 and substantial overestimation as  
509 shown in hydrograph.

510 **Table 2**

511 Evaluation statistics for the performance of eight models in daily streamflow simulation

Precipitation data	Temperature data	Without calibration						After calibration					
		2000-2003			2004-2007			2000-2003 (calibration)			2004-2007 (Validation)		
		NSE	R <sup>2</sup>	PBIAS	NSE	R <sup>2</sup>	PBIAS	NSE	R <sup>2</sup>	PBIAS	NSE	R <sup>2</sup>	PBIAS
Gauge	Gauge	0.49	0.54	-9.80	0.14	0.46	4.40	0.76	0.77	-10.50	0.69	0.75	4.00
	CSFR	0.50	0.54	-9.30	0.16	0.47	2.30	0.78	0.79	-8.00	0.70	0.75	3.60
CHIRPS	Gauge	0.44	0.50	-34.30	0.31	0.44	-26.70	0.56	0.61	-10.50	0.52	0.53	-7.40
	CSFR	0.44	0.49	-33.80	0.31	0.45	-28.70	0.57	0.61	-9.80	0.52	0.54	-8.60
TRMM	Gauge	0.33	0.42	-29.70	0.23	0.38	-38.80	0.49	0.49	-7.40	0.41	0.44	-19.00
	CSFR	0.34	0.42	-29.20	0.24	0.39	-40.40	0.49	0.50	-6.20	0.41	0.44	-20.00
CFSR	Gauge	0.05	0.48	18.90	-1.16	0.51	47.30	0.64	0.67	-18.8	0.01	0.67	20.60
	CSFR	0.05	0.48	19.50	-1.15	0.51	46.20	0.64	0.67	-18.00	0.04	0.67	17.70

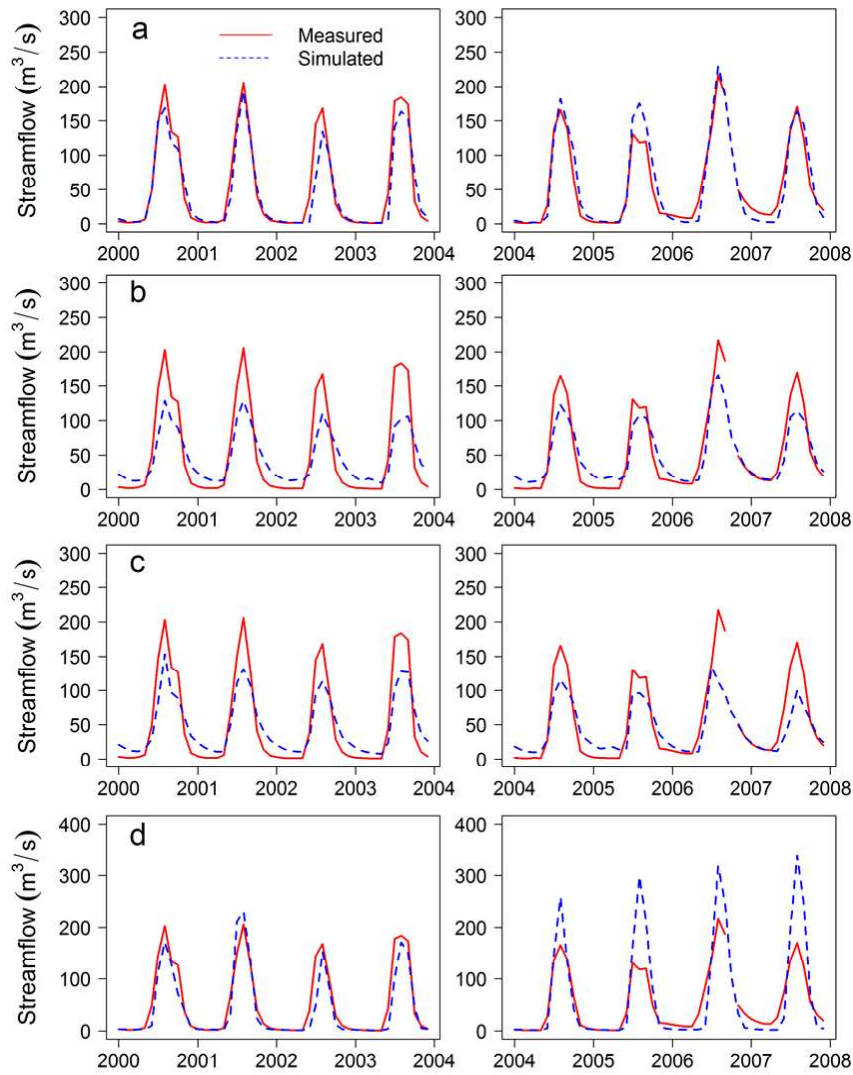
512

513

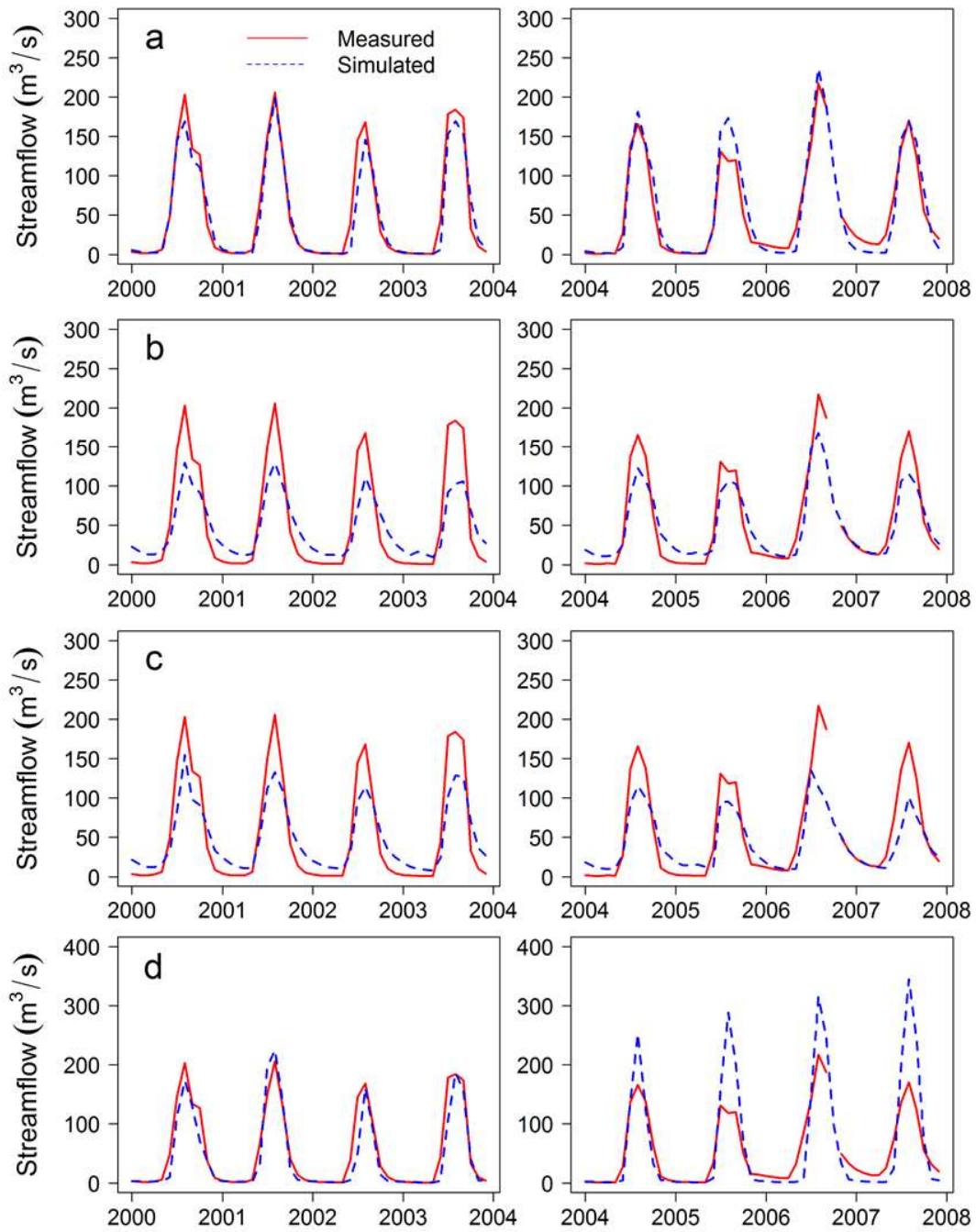
514 **Table 3**

515 Evaluation statistics for the performance of eight models in monthly streamflow simulation

Precipitation data	Temperature data	Without calibration						After calibration					
		2000-2003			2004-2007			2000-2003 (calibration)			2004-2007 (Validation)		
		NSE	R <sup>2</sup>	PBIAS <sub>S</sub>	NSE	R <sup>2</sup>	PBIAS <sub>S</sub>	NSE	R <sup>2</sup>	PBIAS <sub>S</sub>	NSE	R <sup>2</sup>	PBIAS
Gauge	Gauge	0.90	0.93	-9.80	0.93	0.94	4.40	0.92	0.94	-10.50	0.92	0.94	4.10
	CSFR	0.90	0.93	-9.30	0.94	0.94	2.20	0.94	0.95	-8.00	0.92	0.95	3.70
CHIRPS	Gauge	0.68	0.89	-34.30	0.82	0.91	-26.50	0.71	0.88	-10.20	0.85	0.91	-6.60
	CSFR	0.69	0.89	-33.80	0.82	0.92	-28.50	0.72	0.88	-9.50	0.85	0.91	-7.80
TRMM	Gauge	0.77	0.93	-29.70	0.64	0.83	-38.70	0.80	0.92	-7.10	0.72	0.85	-18.30
	CSFR	0.77	0.93	-29.10	0.64	0.85	-40.40	0.80	0.92	-6.00	0.72	0.86	-19.30
CFSR	Gauge	0.81	0.88	18.70	0.07	0.87	46.30	0.86	0.88	-18.80	0.26	0.85	20.60
	CSFR	0.81	0.89	19.40	0.07	0.87	45.10	0.87	0.89	-18.00	0.29	0.85	17.80



517 **Fig. 9.** Comparison of monthly measured and simulated streamflow from models using gauge air  
518 temperature and four different precipitation datasets (a: Gauge, b: CHIRPS, c: TRMM, d: CFSR)  
519 for the calibration period 2000-2003 and validation period 2004-2007.



520



521 **Fig. 10.** Comparison of monthly measured and simulated streamflow from models using CFSR  
522 air temperature and four different precipitation datasets (a: Gauge, b: CHIRPS, c: TRMM, d:  
523 CFSR) for the calibration period 2000-2003 and validation period 2004-2007.

524 In summary, we can conclude that using different precipitation datasets as inputs to SWAT had  
525 much larger influence on streamflow simulation than using different air temperature datasets in  
526 this area. Using CFSR air temperature can yield equal performance to using gauge air  
527 temperature in driving SWAT model in this study area. This is a good news for researches who  
528 are interested in this study area given the limited availability and large amount of gaps in the  
529 gauge air temperature data as mentioned in Section 3.1. About the selection of precipitation  
530 dataset, this study showed that overall measured precipitation from gauge stations (even though  
531 with limited availability and sparse coverage) are still the one that yielded the best simulation  
532 result in this study area. This finding is consistent with other studies (Dile & Srinivasan, 2014;  
533 Tuo et al., 2016; Worqlul et al., 2015; Yang et al., 2014) which reported better performance  
534 using gauge precipitation or interpolation of gauge data than other gridded products. However,  
535 the open-access high resolution gridded products CHIRPS was found to yield satisfactory  
536 performance in daily and monthly streamflow simulation, and thus it can be a good choice in this  
537 study area. In addition, in the case of no access to gauge data at all, the combination of CHIRPS  
538 precipitation and CFSR air temperature can be used as an alternative data source to drive  
539 hydrological model in streamflow simulation in this data-scarce area.

#### 540 4.2.3 Comparison of calibrated parameters

541 Table 4 presents the optimal values of the calibration parameters for all eight models after  
542 calibration using SWAT-CUP. Models using air temperature from gauge and CFSR had exactly

543 the same values if they used the same precipitation data except for using the gauge precipitation.  
544 The models using gauge precipitation but different air temperature data had different optimal  
545 parameter sets, but after careful examination, we found that both parameter sets were ranked as  
546 top two parameters sets with very slight difference in the NSE value. In other words, in the case  
547 of using gauge precipitation as input, when the best parameter set from model using CFSR  
548 temperature was used, the model with gauge temperature could still yield similarly good  
549 performance to that using its own best parameter. This reflects the effect of parameter  
550 equifinality (Beven & Binley, 1992). Interestingly, models with CHIRPS and TRMM  
551 precipitation as input had the same best parameter sets, but using CHIRPS yielded better  
552 performance in daily streamflow simulation (NSE=0.56 and NSE=0.52) than using TRMM  
553 (NSE=0.49 and NSE=0.41) for both calibration and validation periods.

554 **Table 4**

555 Optimal parameters calibrated for all eight models

Parameter s	r_CN 2.mgt	r_SOL_ AWC.sol	v_ES CO.hru	v_GW_D ELAY.gw	v_GW_R EVAP.gw	a_GW QMN.g w	a_REVA PMN.gw	v_CH _K2.rte
GaugeP_ GaugeT	-0.27	0.27	0.95	1.85	0.07	622.43	223.34	7.39
CHIRPSP _GaugeT	0.09	-0.5	0.98	327.18	0.04	285.43	168.56	145.33
TRMMP_ GaugeT	0.09	-0.5	0.98	327.18	0.04	285.43	168.56	145.33
CFSRP_G augeT	-0.28	0.12	0.67	1.88	0.13	3581.52	-280.59	4.72
GaugeP_ CFSRT	-0.27	0.09	0.95	1.87	0.03	607.84	154.37	4.35

CHIRPSP _CFSRT	0.09	-0.5	0.98	327.18	0.04	285.43	168.56	145.33
TRMMP _CFSRT	0.09	-0.5	0.98	327.18	0.04	285.43	168.56	145.33
CFSRP_C FSRT	-0.28	0.12	0.67	1.88	0.13	3581.52	-280.59	4.72

556 *Note.* GaugeP\_GaugeT means the model using gauge precipitation and gauge air temperature as  
557 inputs. CHIRPSP\_CFSRT means the model using CHIRPS precipitation dataset and CFSR air  
558 temperature data as inputs, and so forth.

559 Overall, the calibrated parameters using gauge and CFSR precipitation data were similar, and  
560 those using TRMM and CHIRPS precipitation data were similar. For example, both gauge and  
561 CFSR precipitation led to reductions in the parameter CN2 by 27% and 28%, respectively,  
562 while both TRMM and CHIRPS led to slight increase in CN2 by 9%. Increase in CN2 would  
563 result in more runoff by SWAT. For the parameter SOL\_AWC that is responsible for available  
564 water capacity of the soil layer, both gauge and CFSR precipitation led to increase but the  
565 increase was less for CFSR. CHIRPS and TRMM precipitation datasets resulted in decrease in  
566 SOL\_AWC. The decrease in SOL\_AWC would generally result in less runoff (Neitsch et al.,  
567 2011). For the groundwater delay time (GW\_DELAY), gauge and CFSR precipitation had  
568 similarly small values, which will result in more rapid recharge of the shallow aquifer and  
569 discharge to the stream (Radcliffe & Mukundan, 2017). However, CHIRPS and TRMM had very  
570 large value for GW\_DELAY which translates into slow recharge of the shallow aquifer and  
571 discharge to the stream.

572 In summary, during calibration different parameter values were compensating the difference in  
573 precipitation inputs to increase the agreement with measured streamflow at the basin outlet. This

574 might lead to different hydrological components (e.g. surface runoff and groundwater  
575 contribution). Therefore, even though all models can fit well the measured streamflow, the  
576 partition of water balance components can be different among models (Tuo et al., 2016). This is  
577 the inherent limitation of calibrating and validating a model based on only the streamflow at the  
578 basin outlet. Unfortunately, this is a common practice in hydrological modelling because  
579 measurements for other components are often not available. Many studies have already stressed  
580 that simulation of other water balance components from the model that is calibrated with only  
581 outlet streamflow should be used with great caution (Bitew & Gebremichael, 2011). Once data  
582 allows, the multi-variable and multi-site calibration should be performed to overcome this  
583 uncertainty (Tuo et al., 2018). For example, the satellite-based evapotranspiration or soil  
584 moisture data could be considered to constrain calibration together with outlet streamflow. In this  
585 regard, several studies have been carried out to explore the added values of multi-variable in  
586 improving hydrological modelling in other regions (e.g. (Herman et al., 2018)). The same topic  
587 (multi-variable and multi-site calibration) is interesting and within our plan for further study in  
588 this data-scarce basin in Africa.

#### 589 4.3 Discussion with existing studies in the same study area

590 Several studies have been carried out to evaluate the performance of different precipitation  
591 datasets in driving hydrological model (particularly SWAT) in streamflow simulation in the  
592 same basin or region, e.g. Lake Tana Basin and Blue Nile Basin. We discussed our results with  
593 two most relevant previous studies which considered the same precipitation datasets (CFSR and  
594 TRMM) with our study.

595 Bitew and Gebremichael (2011) evaluated four gridded precipitation products at 0.25° spatial  
596 resolution including TRMM3B42 in driving SWAT for daily streamflow simulation in the same  
597 upper Gilgel Abay Basin. The model was calibrated for the period 2003-2004 and validated for  
598 2006-2007. The authors reported only analysis of validation period at daily timescale. They  
599 found that using TRMM3B42 resulted in unsatisfactory daily streamflow simulation with  
600 substantial underestimation. The evaluation statistics showed that  $R^2$  values were 0.50 and less  
601 than 0.2 for 2006 and 2007, respectively, while NSE were 0.16 and negative. Our study found  
602 the same unsatisfactory performance of TRMM in driving SWAT for daily streamflow, which is  
603 in good agreement with Bitew and Gebremichael (2011). However, our evaluation statistics for  
604 using TRMM3B42 were much better. This could be mainly due to two reasons: (1) mostly  
605 importantly *Bitew and Gebremichael* (2011) used old version of TRMM product, while our study  
606 used the latest product. Previous study already showed that latest version performed much better  
607 than previous version and had reasonably good agreement with gauge-based measurements in the  
608 same region (Duan & Bastiaanssen, 2013a). (2) Besides the difference in precipitation data and  
609 other data used for setting up SWAT model, the calibration strategy used by Bitew and  
610 Gebremichael (2011) might not be able to find the optimal values for TRMM3B42, although  
611 they did not explicitly detailed the calibration procedures rather just simply mentioned the  
612 application of automatic and manual calibration. Our study used a more objective calibration  
613 with the same starting parameter ranges in a sufficient number of iterations, which increases the  
614 possibility of finding optimal parameter values for each precipitation product and allow for a  
615 more fair inter-comparison among different precipitation products.

616 Dile and Srinivasan (2014) was perhaps the first study that evaluated the performance of using  
617 CFSR in driving SWAT for streamflow simulation in Lake Tana Basin with the upper Gilgel

618 Abay Basin included. They evaluated the performance of CFSR precipitation and air temperature  
619 in monthly streamflow simulation using SWAT without calibration for the period 1993-2007.  
620 They concluded that using CFSR data yielded satisfactory performance (NSE=0.79) in  
621 simulating monthly streamflow. Our study found that without calibration using CSFR  
622 precipitation and air temperature yielded very good performance (NSE=0.81) in monthly  
623 streamflow simulation for the period 2000-2003, but very poor performance (NSE=0.07) for the  
624 2004-2007. Thus, our finding partially contradicts with their findings. After careful comparison,  
625 we found that as shown in Fig. 1 of Dile and Srinivasan (2014), they somehow consistently  
626 discarded all CFSR data in the western part of the study area, even there are CFSR stations  
627 located within the study area. This is because they used a smaller bounding box (particularly a  
628 larger west longitude value of 36.89°E) than actually needed for covering the entire study area  
629 (the area stretches out to the west longitude value of 36.82°E) when they requested the data from  
630 the CFSR data portal at <https://globalweather.tamu.edu/>. As a result, their study used only two  
631 CFSR stations (P111372 and P114372) but missed inclusion of another two CFSR stations  
632 (P114369 and P111369) that actually should be considered for the upper Gilgel Abay Basin. We  
633 analyzed the precipitation data from all the four CFSR stations and found that the other two  
634 stations have substantially higher amount of precipitation. To be specific, the average daily  
635 precipitation during the period 2000-2007 is 4.8 mm/day for P111372, 2.2 mm/day for P114372,  
636 8.4 mm/day for P111369 and 6.5 mm/day for P114369. Our study used more CFSR stations that  
637 should normally be used, and thus CFSR precipitation resulted in severe overestimation  
638 particularly in the validation period 2004-2007. While Dile and Srinivasan (2014) used two  
639 CFSR stations with lower amount precipitation, and thus better simulation result can be obtained.

640 To further test our speculation and make a proper comparison, we did further analysis: we did  
641 intentionally used the same two CFSR stations as Dile and Srinivasan (2014) did to run SWAT  
642 model, and we further considered results without calibration as well as after calibration. Table 5  
643 shows the evaluation statistics for performance of streamflow simulation using precipitation and  
644 air temperature from only two CFSR stations. Without calibration, the monthly streamflow  
645 simulation showed very good performance with NS of 0.76 for both calibration and validation  
646 period, which is now in agreement with conclusion by Dile and Srinivasan (2014). This confirms  
647 our speculation. However, strictly speaking, the evaluation by Dile and Srinivasan (2014) did not  
648 reflect the complete accuracy of CFSR because of the unintentionally exclusion of two stations.  
649 It should be noted that normally users of CFSR will use a larger box covering entirely the study  
650 area to select data like what we did in this study, then the good results reported by Dile and  
651 Srinivasan (2014) cannot be reproduced. In addition, without ground measurements as reference,  
652 pre-selection of CFSR stations cannot be performed in a favorable manner.

653 **Table 5**

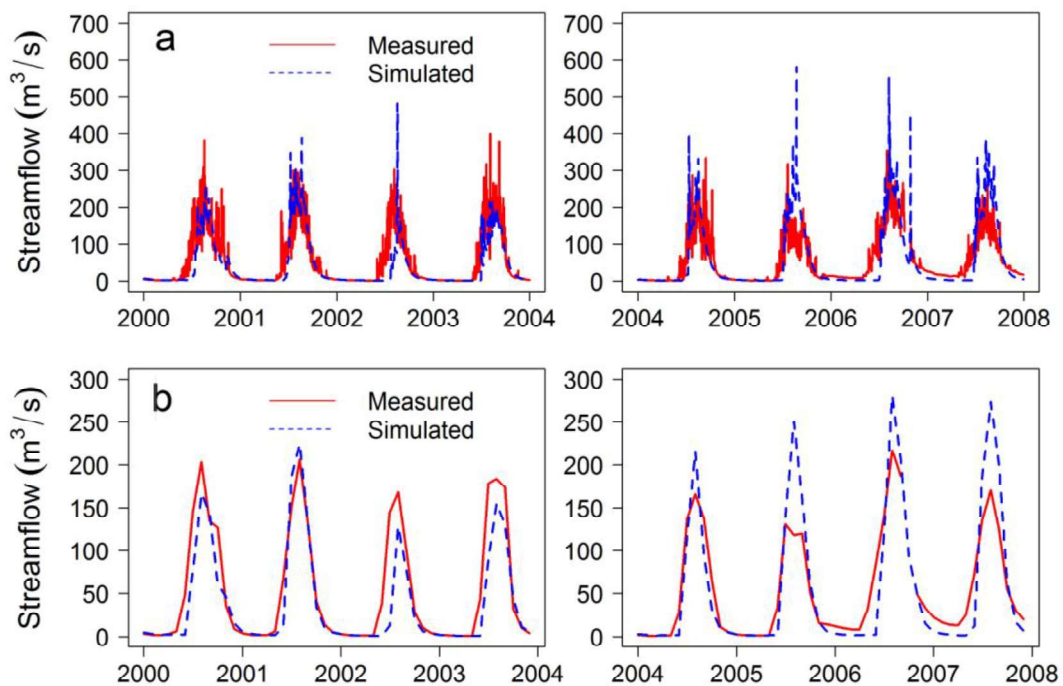
654 Evaluation statistics for the performance of model using air temperature and precipitation from  
655 only two CFSR stations as Dile and Srinivasan (2014) did in daily and monthly streamflow  
656 simulation

Timescale	Without calibration						After calibration					
	2000-2003			2004-2007			2000-2003 (calibration)			2004-2007 (Validation)		
	NSE	R <sup>2</sup>	PBIAS	NSE	R <sup>2</sup>	PBIAS	NSE	R <sup>2</sup>	PBIAS	NSE	R <sup>2</sup>	PBIAS
Daily	0.13	0.34	-27.30	-0.35	0.41	0.10	0.56	0.60	-25.80	0.36	0.66	2.30
Monthly	0.76	0.82	-27.40	0.76	0.86	-1.50	0.77	0.81	-25.80	0.63	0.85	2.00

657

658 Furthermore, our analysis showed that without calibration using the only two stations from  
659 CFSR still performed unsatisfactorily for daily streamflow with NSE of 0.13 and -0.35 in the

660 calibration and validation periods, respectively. This suggests that the reported good  
661 performance of a certain precipitation at monthly timescale does not necessarily guarantee the  
662 equally good performance at finer timescale (e.g. daily). Local community should pay due  
663 attention to this issue when selecting precipitation products. Even after performing the same  
664 calibration strategy, the data from only two CFSR stations can yield satisfactory performance  
665 (NSE=0.56) in daily streamflow simulation for the calibration period but fail to generate  
666 satisfactory for the validation period (NSE=0.36). Fig. 11 shows the comparison of simulated  
667 and measured streamflow at daily and monthly timescale. Therefore, taken together, considering  
668 both calibration and validation periods, CFSR precipitation data is not a good alternative data  
669 source in this study area. By contrast, CHIRPS precipitation data yielded more consistent  
670 performance and the performance was as good as (if not better than) CFSR in daily and monthly  
671 streamflow simulation.



672



673 **Fig. 11.** Comparison of daily (the top panel a) and monthly (the bottom panel b) measured and  
674 simulated streamflow from model using air temperature and temperature data from only two  
675 CFSR stations as (Dile and Srinivasan, 2014) did for the calibration period 2000-2003 and  
676 validation period 2004-2007.

677

#### 678 4.4 General discussion and recommendations for future study

679 Overall the CHIRPS precipitation outperformed TRMM and CFSR precipitation products in  
680 driving SWAT model for streamflow simulation in this study. The CFSR product tended to  
681 overestimate precipitation and yielded unsatisfactory streamflow simulation using SWAT.  
682 Similar significant overestimation of CFSR precipitation data have also been reported in many  
683 other regions with different sizes and environmental conditions, e.g. Singapore (Tan et al., 2018),  
684 two basins in Malaysia (Tan et al., 2017), several basins in China (Zhu et al., 2016; Gao et al.,  
685 2018a), the Mekong River Basin (Chen et al., 2018), and six basins in West Africa (Poméon et  
686 al., 2017). It seems that only a limited number of studies reported the reasonable performance of  
687 CFSR precipitation, e.g. in four small basins in USA and the Gumera basin in Ethiopia (Fuka et  
688 al., 2014). This suggests that the large uncertainty of CFSR precipitation product and it should be  
689 used with great cautions. In contrast, literature search showed a very limited number of studies  
690 that evaluated the performance of CFSR air temperature. One existing study by Tan et al. (2017)  
691 found good correlation of CFSR air temperature product with in-situ measurements in two basins  
692 in Malaysia and further using CFSR air temperature can yield good streamflow simulation using  
693 SWAT. Their findings are consistent with ours in the current study.

694

695 Since the CHIRPS precipitation product (released in 2015) is a relatively new product, thus there  
696 are a relatively small number (around 30 journal publications) of studies on the assessment of  
697 CHIRPS product and comparison with other widely used products such as TRMM. It is  
698 interesting to mention that similar to our study many studies have reported that CHIRPS product  
699 has good performance being comparably good or even better than TRMM product, for example,  
700 in Mozambique (Toté et al., 2015), Adige basin in Italy (Duan et al., 2016), Upper Blue Nile  
701 (Bayissa et al., 2017), East Africa (Kimani et al., 2017, Gebrechorkos et al., 2018), West Africa  
702 (Poméon et al., 2017) and Haihe River Basin, China (Gao et al., 2018). After a comprehensive  
703 global evaluation of 22 precipitation products, Beck et al. (2017) also concluded that CHIRPS is  
704 a viable choice for tropical regions.

705

706 It should be noted that this study only evaluated the performance of the CHIRPS, TRMM and  
707 CFSR precipitation products and CFSR air temperature at the daily and monthly scales. The  
708 CHIRPS stands out in terms of finer spatial resolution ( $0.05^\circ$ ), but it only provides daily  
709 precipitation product. The TRMM and CFSR products with sub-daily temporal resolutions are  
710 expected to have beneficial potentials for applications that require precipitation and streamflow  
711 simulation at sub-daily scales, e.g. flood simulation. We recommend to evaluate performances of  
712 multiple gridded precipitation products at sub-daily scales in future studies. One particular  
713 product to evaluate is the Global Precipitation Measurement (GPM) product, the Integrated  
714 Multi-satellite Retrievals for GPM (IMERG) became available from March 2014, due to its high  
715 temporal (30-minute) and spatial resolution ( $0.1^\circ$ ) (Yuan et al. 2018).

## 716 **5 Conclusions**

717 Motivated by the scarcity and substantial temporal and spatial gaps in ground measurements in  
718 many basins in Africa, this study evaluated the performance of using three open-access  
719 precipitation datasets (CHIRPS, TRMM and CFSR) and one air temperature dataset (CFSR) in  
720 driving SWAT model in simulation of daily and monthly streamflow in the upper Gilgel Abay  
721 Basin, Ethiopia. The “best” available measurements of precipitation and air temperature from  
722 sparse gauge stations were also used to drive SWAT model and the results were compared with  
723 those using open-access datasets. After a comprehensive comparison of a total of eight model  
724 scenarios, we can draw the following conclusions.

725 (1) Using measured precipitation from even sparse available stations consistently yielded  
726 better performance in streamflow simulation than using all three open-access  
727 precipitation datasets, and thus all three open-access precipitation datasets cannot be  
728 substitute for ground measurements.

729 (2) Using CFSR air temperature yielded almost identical performance in streamflow  
730 simulation to using measured air temperature from gauge stations. This suggests the  
731 favorable accuracy of CFSR air temperature to use for hydrological modelling in this  
732 region. This is a good news for the local community as the availability and quality of  
733 measured air temperature is often worse than that of precipitation.

734 (3) Among the three precipitation datasets, overall CHIRPS yielded the best performance and  
735 it was the only one that can achieve satisfactory simulation of daily streamflow. The  
736 recommended CFSR precipitation by previous study consistently overestimated

737 precipitation and using CFSR precipitation resulted in inconsistent and overall  
738 unsatisfactory performance in daily and monthly streamflow simulation.

739 (4) Even without calibration, using CHIRPS and TRMM precipitation datasets comparably  
740 resulted in satisfactory and up to very good performance in monthly streamflow  
741 simulation. This further demonstrates the applicability of SWAT model in this study area  
742 and the reasonable accuracy of the two datasets at the monthly timescale.

743 (5) Using different precipitation datasets resulted in different best parameters during  
744 calibration. Therefore, simulation of other water balance components from the model that  
745 is calibrated with only outlet streamflow should be used with great caution, as also  
746 stressed by Bitew and Gebremichael (2011). Multi-variable and multi-site calibration is a  
747 promising way to overcome this limitation to a certain degree.

748 (6) Taken together, the CHIRPS precipitation available at high spatial resolution (0.05°)  
749 together with CFSR air temperature can be a promising alternative open-access data  
750 source for streamflow simulation with SWAT in this data-scarce area in the case of  
751 limited access to desirable gauge data.

752 Due to non-availability of gauged wind speed, solar radiation and relative humidity, this study  
753 did not explore the performance of using complete CFSR weather data in driving SWAT. The  
754 complete CFSR weather data enable users to use the other two more data-demanding methods  
755 for calculating potential evapotranspiration. Previous studies showed that different methods  
756 resulted in large different potential evapotranspiration estimates and further had certain effects  
757 on streamflow simulation by SWAT (Samadi, 2017). This is an interesting topic for future study.  
758 In addition, future studies can also include further testing of CHIRPS data in more different

759 regions, and the added values of currently available satellite products in constraining calibration  
760 and spatially evaluation of hydrological models particularly in poorly and even ungauged basins.

## 761 **Acknowledgments**

762 We thank all providers as specified in Section 3 of this manuscript for providing datasets for this  
763 study. This work was supported by National Basic Research Program of China (Project No.:  
764 2015CB954102), Natural Science Foundation of Jiangsu Province of China (Project No.:  
765 BK20150975), National Natural Science Foundation of China (Project No.: 41601413,  
766 41431177), PAPD (Project No.: 164320H116), and Program of Innovative Research Team of  
767 Jiangsu Higher Education Institutions of China. We would like to thank two anonymous  
768 reviewers and the Editor for constructive comments which helped improve the quality of this  
769 paper.

## 770 **References**

- 771 Abbaspour, K., 2015. SWAT-CUP 2012: SWAT calibration and uncertainty programs: A user manual.  
772 Department of Systems Analysis, Integrated Assessment and Modelling (SIAM), Eawag, Swiss Federal  
773 Institute of Aquatic Science and Technology, Duebendorf, Switzerland.
- 774 Abbaspour, K.C., Johnson, C.A., Genuchten, M.T.V., 2004. Estimating Uncertain Flow and Transport  
775 Parameters Using a Sequential Uncertainty Fitting Procedure. *Vadose Zone Journal*, 3(4): 1340-1352.
- 776 Abbaspour, K.C. et al., 2015. A continental-scale hydrology and water quality model for Europe: Calibration  
777 and uncertainty of a high-resolution large-scale SWAT model. *Journal of Hydrology*, 524: 733-752.
- 778 Abbaspour, K.C. et al., 2007. Modelling hydrology and water quality in the pre-alpine/alpine Thur watershed  
779 using SWAT. *Journal of Hydrology*, 333(2): 413-430.

- 780 Arnold, J.G., Fohrer, N., 2005. SWAT2000: current capabilities and research opportunities in applied  
781 watershed modelling. *Hydrological Processes*, 19(3): 563-572.
- 782 Arnold, J.G., Srinivasan, R., Muttiah, R.S., Williams, J.R., 1998. LARGE AREA HYDROLOGIC  
783 MODELING AND ASSESSMENT PART I: MODEL DEVELOPMENT. *Jawra Journal of the American*  
784 *Water Resources Association*, 34(1): 73-89.
- 785 Awange, J. et al., 2016. Uncertainties in remotely sensed precipitation data over Africa. *International Journal*  
786 *of Climatology*, 36(1): 303-323.
- 787 Bayissa, Y., Tadesse, T., Demisse, G., Shiferaw, A., 2017. Evaluation of Satellite-Based Rainfall Estimates  
788 and Application to Monitor Meteorological Drought for the Upper Blue Nile Basin, Ethiopia. *Remote*  
789 *Sensing*, 9(7): 669.
- 790 Beck, H.E. et al., 2017. Global-scale evaluation of 22 precipitation datasets using gauge observations and  
791 hydrological modeling. *Hydrology and Earth System Sciences*, 21(12): 6201-6217.
- 792 Beven, K., Binley, A., 1992. The future of distributed models: Model calibration and uncertainty prediction.  
793 *Hydrological Processes*, 6(3): 279-298.
- 794 Bitew, M., Gebremichael, M., 2011. Assessment of satellite rainfall products for streamflow simulation in  
795 medium watersheds of the Ethiopian highlands. *Hydrology and Earth System Sciences*, 15(4): 1147.
- 796 Chen, A., Chen, D., Azorin-Molina, C., 2018. Assessing reliability of precipitation data over the Mekong  
797 River Basin: A comparison of ground-based, satellite, and reanalysis datasets. *International Journal of*  
798 *Climatology*, 38(11): 4314-4334.
- 799 Dile, Y.T., Srinivasan, R., 2014. Evaluation of CFSR climate data for hydrologic prediction in data-scarce  
800 watersheds: An application in the blue Nile river basin. *Journal of the American Water Resources*  
801 *Association*, 50(5): 1226-1241. DOI:10.1111/jawr.12182
- 802 Duan, Z., Bastiaanssen, W., 2013a. First results from Version 7 TRMM 3B43 precipitation product in  
803 combination with a new downscaling–calibration procedure. *Remote Sensing of Environment*, 131: 1-13.

804 Duan, Z., Bastiaanssen, W.G.M., 2013b. Estimating water volume variations in lakes and reservoirs from four  
805 operational satellite altimetry databases and satellite imagery data. *Remote Sensing of Environment*, 134(5):  
806 403-416.

807 Duan, Z., Bastiaanssen, W., Liu, J., 2012a. Monthly and annual validation of TRMM Multisatellite  
808 Precipitation Analysis (TMPA) products in the Caspian Sea Region for the period 1999–2003, *Geoscience  
809 and Remote Sensing Symposium (IGARSS)*, 2012 IEEE International. IEEE, pp. 3696-3699.

810 Duan, Z., Bastiaanssen, W.G.M., Liu, J., 2012b. Monthly and annual validation of TRMM Multisatellite  
811 Precipitation Analysis (TMPA) products in the Caspian Sea Region for the period 1999–2003, *Geoscience  
812 and Remote Sensing Symposium*, pp. 3696-3699.

813 Duan, Z., Liu, J., Tuo, Y., Chiogna, G., Disse, M., 2016. Evaluation of eight high spatial resolution gridded  
814 precipitation products in Adige Basin (Italy) at multiple temporal and spatial scales. *Science of The Total  
815 Environment*, 573: 1536-1553.

816 Fuka, D.R. et al., 2014. Using the Climate Forecast System Reanalysis as weather input data for watershed  
817 models. *Hydrological Processes*, 28(22): 5613-5623.

818 Funk, C. et al., 2015. The climate hazards infrared precipitation with stations—a new environmental record for  
819 monitoring extremes. *Scientific Data*, 2(9): 150066.

820 Gao, X., Zhu, Q., Yang, Z., Wang, H., 2018a. Evaluation and hydrological application of CMADS against  
821 TRMM 3B42V7, PERSIANN-CDR, NCEP-CFSR, and gauge-based datasets in Xiang River basin of China.  
822 *Water (Switzerland)*, 10(9).

823 Gao, F. et al., 2018b. Evaluation of CHIRPS and its application for drought monitoring over the Haihe River  
824 Basin, China. *Natural Hazards*, 92(1): 155-172.

825 Gassman, P.W., Reyes, M.R., Green, C.H., Arnold, J.G., 2007. The soil and water assessment tool: historical  
826 development, applications, and future research directions. *Transactions of the ASABE*, 50(4): 1211-1250.

- 827 Gebrechorkos, S.H., Hülsmann, S., Bernhofer, C., 2018. Evaluation of multiple climate data sources for  
828 managing environmental resources in East Africa. *Hydrology and Earth System Sciences*, 22(8): 4547-4564.
- 829 Griensven, A.v., Ndomba, P., Yalew, S., Kilonzo, F., 2012. Critical review of SWAT applications in the upper  
830 Nile basin countries. *Hydrology and Earth System Sciences*, 16(9): 3371-3381.
- 831 Green, W.H., Ampt, G. A., 1911. Studies on Soil Physics. *The Journal of Agricultural Science*, 4(1), 11-24.
- 832 Hargreaves, G.H., Samani, Z.A., 1982. Estimating potential evapotranspiration. *Journal of the Irrigation &*  
833 *Drainage Division*, 108(3): 225-230.
- 834 Herman, M.R. et al., 2018. Evaluating the role of evapotranspiration remote sensing data in improving  
835 hydrological modeling predictability. *Journal of Hydrology*, 556: 39-49.
- 836 Hrachowitz, M. et al., 2013. Decade of Predictions in Ungauged Basins (PUB)-a review. *Hydrological*  
837 *Sciences Journal*, 58(6), 1198-1255.
- 838 Huffman, G.J. et al., 2007. The TRMM multisatellite precipitation analysis (TMPA): Quasi-global, multiyear,  
839 combined-sensor precipitation estimates at fine scales. *Journal of hydrometeorology*, 8(1): 38-55.
- 840 Jiang, S. et al., 2017. Hydrologic Evaluation of Six High Resolution Satellite Precipitation Products in  
841 Capturing Extreme Precipitation and Streamflow over a Medium-Sized Basin in China. *Water*, 10(1): 25.
- 842 Kimani, M.W., Hoedjes, J.C.B., Su, Z., 2017. An assessment of satellite-derived rainfall products relative to  
843 ground observations over East Africa. *Remote Sensing*, 9(5).
- 844 Laiti, L. et al., Testing the Hydrological Coherence of High- Resolution Gridded Precipitation and  
845 Temperature Data Sets. *Water Resources Research*.
- 846 Liu, J., Duan, Z., Jiang, J., Zhu, A., 2015. Evaluation of three satellite precipitation products TRMM 3B42,  
847 CMORPH, and PERSIANN over a subtropical watershed in China. *Advances in Meteorology*, 2015.
- 848 Mekonnen, D.F., Duan, Z., Rientjes, T., Disse, M., 2018. Analysis of combined and isolated effects of land-use  
849 and land-cover changes and climate change on the upper Blue Nile River basin's streamflow. *Hydrology*  
850 *and Earth System Sciences*, 22: 6187-6207.



- 851 Moriasi, D.N. et al., 2007. Model evaluation guidelines for systematic quantification of accuracy in watershed  
852 simulations. *Transactions of the Asabe*, 50(3): 885-900.
- 853 Nash, J.E., Sutcliffe, J.V., 1970. River flow forecasting through conceptual models part I — A discussion of  
854 principles ☆. *Journal of Hydrology*, 10(3): 282-290.
- 855 Poméon, T., Jackisch, D., Diekkrüger, B., 2017. Evaluating the performance of remotely sensed and  
856 reanalysed precipitation data over West Africa using HBV light. *Journal of Hydrology*, 547: 222-235.
- 857 Radcliffe, D.E., Mukundan, R., 2017. PRISM vs. CFSR Precipitation Data Effects on Calibration and  
858 Validation of SWAT Models. *Journal of the American Water Resources Association*, 53(1): 89-100.  
859 DOI:10.1111/1752-1688.12484
- 860 Roth, V., Lemann, T., 2016. Comparing CFSR and conventional weather data for discharge and soil loss  
861 modelling with SWAT in small catchments in the Ethiopian Highlands. *Hydrology and Earth System  
862 Sciences*, 20(2): 921-934. DOI:10.5194/hess-20-921-2016
- 863 Saha, S. et al., 2010. The NCEP climate forecast system reanalysis. *Bulletin of the American Meteorological  
864 Society*, 91(8): 1015-1058.
- 865 Samadi, S.Z., 2017. Assessing the sensitivity of SWAT physical parameters to potential evapotranspiration  
866 estimation methods over a coastal plain watershed in the southeastern United States. *Hydrology Research*,  
867 48(2): 395-415.
- 868 Setegn, S.G., Srinivasan, R., Melesse, A.M., Dargahi, B., 2010. SWAT model application and prediction  
869 uncertainty analysis in the Lake Tana Basin, Ethiopia. *Hydrological Processes*, 24(3): 357-367.
- 870 Song, X., Duan, Z., Kono, Y., Wang, M., 2011. Integration of remotely sensed C factor into SWAT for  
871 modelling sediment yield. *Hydrological Processes*, 25(22): 3387-3398.
- 872 Tan, M.L., Chua, V.P., Tan, K.C., Brindha, K., 2018. Evaluation of TMPA 3B43 and NCEP-CFSR  
873 precipitation products in drought monitoring over Singapore. *International Journal of Remote Sensing*,  
874 39(8): 2089-2104.

- 875 Tan, M.L., Duan, Z., 2017. Assessment of GPM and TRMM precipitation products over singapore. Remote  
876 Sensing, 9(7): 720
- 877 Tan, M.L., Gassman, P.W., Cracknell, A.P., 2017. Assessment of three long-term gridded climate products for  
878 hydro-climatic simulations in tropical river basins. Water, 9(3)..
- 879 Tang, G., Ma, Y., Long, D., Zhong, L., Hong, Y., 2016. Evaluation of GPM Day-1 IMERG and TMPA  
880 Version-7 legacy products over Mainland China at multiple spatiotemporal scales. Journal of Hydrology,  
881 533: 152-167.
- 882 Tapiador, F.J. et al., 2012. Global precipitation measurement: Methods, datasets and applications. Atmospheric  
883 Research, 104-105(1): 70-97.
- 884 Taye, M.T., Willems, P., 2012. Temporal variability of hydroclimatic extremes in the Blue Nile basin. Water  
885 Resources Research, 48(3): 3513.
- 886 Tekleab, S. et al., 2011. Water balance modeling of Upper Blue Nile catchments using a top-down approach.  
887 Hydrology and Earth System Sciences, 15(7): 2179.
- 888 Toté, C. et al., 2015. Evaluation of satellite rainfall estimates for drought and flood monitoring in Mozambique.  
889 Remote Sensing, 7(2): 1758-1776.
- 890 Tuo, Y., Duan, Z., Disse, M., Chiogna, G., 2016. Evaluation of precipitation input for SWAT modeling in  
891 Alpine catchment: A case study in the Adige river basin (Italy). Science of the Total Environment, 573: 66-  
892 82.
- 893 Tuo, Y., Marcolini, G., Disse, M., Chiogna, G., 2018. A Multi-Objective Approach to Improve SWAT Model  
894 Calibration in Alpine Catchments. Journal of Hydrology.
- 895 Uhlenbrook, S., Mohamed, Y., Gragne, A., 2010. Analyzing catchment behavior through catchment modeling  
896 in the Gilgel Abay, upper Blue Nile River basin, Ethiopia. Hydrology and Earth System Sciences, 14(10):  
897 2153-2165.

898 USDA-SCS, 1972. SCS national engineering handbook, section 4: hydrology. US Department of Agriculture,  
899 Washington, DC.

900 Wagner, P.D., Fiener, P., Wilken, F., Kumar, S., Schneider, K., 2012. Comparison and evaluation of spatial  
901 interpolation schemes for daily rainfall in data scarce regions. *Journal of Hydrology*, 464-465(5): 388-400.

902 Wale, A., Rientjes, T.H.M., Gieske, A.S.M., Getachew, H.A., 2009. Ungauged catchment contributions to  
903 Lake Tana's water balance. *Hydrological Processes*, 23(26): 3682-3693.

904 Worqlul, A.W. et al., 2014. Comparison of rainfall estimations by TRMM 3B42, MPEG and CFSR with  
905 ground-observed data for the Lake Tana basin in Ethiopia. *Hydrology and Earth System Sciences*, 18(12):  
906 4871-4881.

907 Yang, J., Reichert, P., Abbaspour, K.C., Xia, J., Yang, H., 2008. Comparing uncertainty analysis techniques  
908 for a SWAT application to the Chaohe Basin in China. *Journal of Hydrology*, 358(1-2): 1-23.

909 Yang, Y., Wang, G., Wang, L., Yu, J., Xu, Z., 2014. Evaluation of gridded precipitation data for driving  
910 SWAT model in area upstream of three gorges reservoir. *PloS one*, 9(11): e112725.

911 Ye, T., Marcolini, G., Disse, M., Chiogna, G., 2018. A Multi-Objective Approach to Improve SWAT Model  
912 Calibration in Alpine Catchments. *Journal of Hydrology*.

913 Yong, B. et al., 2010. Hydrologic evaluation of Multisatellite Precipitation Analysis standard precipitation  
914 products in basins beyond its inclined latitude band: A case study in Laohahe basin, China. *Water  
915 Resources Research*, 46(7).

916 Yuan, F. et al., 2018. Evaluation of hydrological utility of IMERG Final run V05 and TMPA 3B42V7 satellite  
917 precipitation products in the Yellow River source region, China. *Journal of Hydrology*. In Press.

918 Zambrano-Bigiarini, M., 2014. hydroGOF: Goodness-of-fit functions for comparison of simulated and  
919 observed hydrological time series. R package version 0.3-8.

920 Zhu, Q., Xuan, W., Liu, L., Xu, Y.P., 2016. Evaluation and hydrological application of precipitation estimates  
921 derived from PERSIANN-CDR, TRMM 3B42V7, and NCEP-CFSR over humid regions in China.  
922 Hydrological Processes, 30(17): 3061-3083.